nature cell biology

A TAG1-APP signalling pathway through Fe65 negatively modulates neurogenesis

Quan-Hong Ma[1,2,3,4], Toshitaka Futagawa[2,5,13], Wu-Lin Yang[2,13], Xiao-Dan Jiang[6], Li Zeng[1], Yasuo Takeda[5], Ru-Xiang Xu[6], Dominique Bagnard[4], Melitta Schachner[3,7], Andrew J. Furley[8], Domna Karagogeos[9], Kazutada Watanabe[10], Gavin S. Dawe[11,14] and Zhi-Cheng Xiao[1,2,12,14]

The release of amyloid precursor protein (APP) intracellular domain (AICD) may be triggered by extracellular cues through γ-secretase-dependent cleavage. AICD binds to Fe65, which may have a role in AICD-dependent signalling; however, the functional ligand has not been characterized. In this study, we have identified TAG1 as a functional ligand of APP. We found that, through an extracellular interaction with APP, TAG1 increased AICD release and triggered Fe65-dependent activity in a γ-secretase-dependent manner. TAG1, APP and Fe65 colocalized in the neural stem cell niche of the fetal ventricular zone. Neural precursor cells from *TAG1*$^{-/-}$, *APP*$^{-/-}$ and *TAG1*$^{-/-}$;*APP*$^{-/-}$ mice had aberrantly enhanced neurogenesis, which was significantly reversed in *TAG1*$^{-/-}$ mice by TAG1 or AICD but not by AICD mutated at the Fe65 binding site. Notably, TAG1 reduced normal neurogenesis in *Fe65*$^{+/+}$ mice. Abnormally enhanced neurogenesis also occurred in *Fe65*$^{-/-}$ mice but could not be reversed by TAG1. These results describe a TAG1–APP signalling pathway that negatively modulates neurogenesis through Fe65.

The γ-secretase proteolytic complex cleaves a wide spectrum of type-1 transmembrane protein substrates, including Notch and APP, by regulated intramembrane proteolysis (RIP) to release their intracellular domains[1]. Ligand-binding to the substrate protein is one mechanism by which this cleavage is regulated. When a ligand binds to Notch, RIP stimulates the release of the intracellular domain of Notch (NICD), which interacts with the transcription factor CSL (CBF1, Suppressor of Hairless and Lag1; ref. 1). Similar transcriptional activity or regulation has been proposed for the intracellular domains cleaved from other γ-secretase substrates, including AICD, which is cleaved from APP[1]. It is therefore important to understand the physiological mechanisms regulating cleavage of AICD.

Glycophosphatidylinositol (GPI)-linked proteins are anchored to the outer leaflet of the plasma membrane and mediate the dynamic remodelling of membranes during cell–cell interactions. In the central nervous system (CNS), GPI-linked recognition molecules, such as TAG1, NB-3 and F3, have been implicated in key developmental events, including selective axonal fasciculation, neural cell adhesion and migration, and neurite outgrowth[2]. Recently, we identified F3 and its homologue NB-3 as functional ligands for the Notch receptor and we showed that their interaction with each other is involved in oligodendrocyte differentiation through activation of the transcriptional factor Deltex1 (refs 3, 4). Given that RIP processing of APP is strikingly similar to that of the Notch receptor[5], knowledge of the interaction between F3 and the Notch receptor has led us to ask whether members of the F3 family may act as APP ligands.

RESULTS

TAG1 and APP bind to each other

To investigate the potential interaction between APP and members of the F3 subfamily, cell adhesion assays were performed. When F3-transfected CHO (CHOF3) cells or non-transfected CHO cells were seeded onto culture dishes spotted with APP–Fc (recombinant APP extracellular domain in fusion with the Fc part of immunoglobulin), little adhesion was observed (Fig. 1a). However, when CHO cells transfected with TAG1 (CHOTAG1), or TAX (the human homologue of TAG1; CHOTAX; data not shown), were seeded onto culture dishes spotted with APP–Fc, the cells readily adhered to the APP protein spots

[1]Institute of Molecular and Cell Biology, 61 Biopolis Drive, Proteos, Singapore138673. [2]Department of Clinical Research, Singapore General Hospital, Singapore 169608. [3]Zentrum fur Molekulare Neurobiologie, University of Hamburg, D-20251 Hamburg, Germany. [4]INSERM U575, Physiopathologie du Systeme Nerveux, Centre de Neurochimie, 67084 Strasbourg, France. [5]Department of Clinical Pharmacy and Pharmacology, Kagoshima University Graduate School of Medical and Dental Sciences, Kagoshima 890-8520, Japan. [6]Neuromedical Institute, Zhujiang Hospital of Southern Medical University, Guangzhou, 510282, China. [7]Keck Center for Collaborative Neuroscience, Rutgers University, Piscataway, NJ 08854-6999, USA. [8]Centre for Developmental Genetics, School of Medicine and Biomedical Science, University of Sheffield, Western Bank, Sheffield S10 2TN, UK. [9]Institute of Molecular Biology and Biotechnology and University of Crete Medical School, Heraklion 71110, Crete, Greece. [10]Department of Bioengineering, Nagaoka University of Technology, Nagaoka 940-2188, Japan. [11]Department of Pharmacology and [12]Department of Anatomy, Yong Loo Lin School of Medicine, National University of Singapore, Singapore117597.
[13]These authors contributed equally to the work.
[14]Correspondence should be addressed to Z.-C.X. or G.S.D. (e-mail: xiao.zhi.cheng@sgh.com.sg; gavindawe@nus.edu.sg)

Received 22 November 2007; accepted 21 January 2008; published online 17 February 2008; DOI: 10.1038/ncb1690

© 2008 Nature Publishing Group

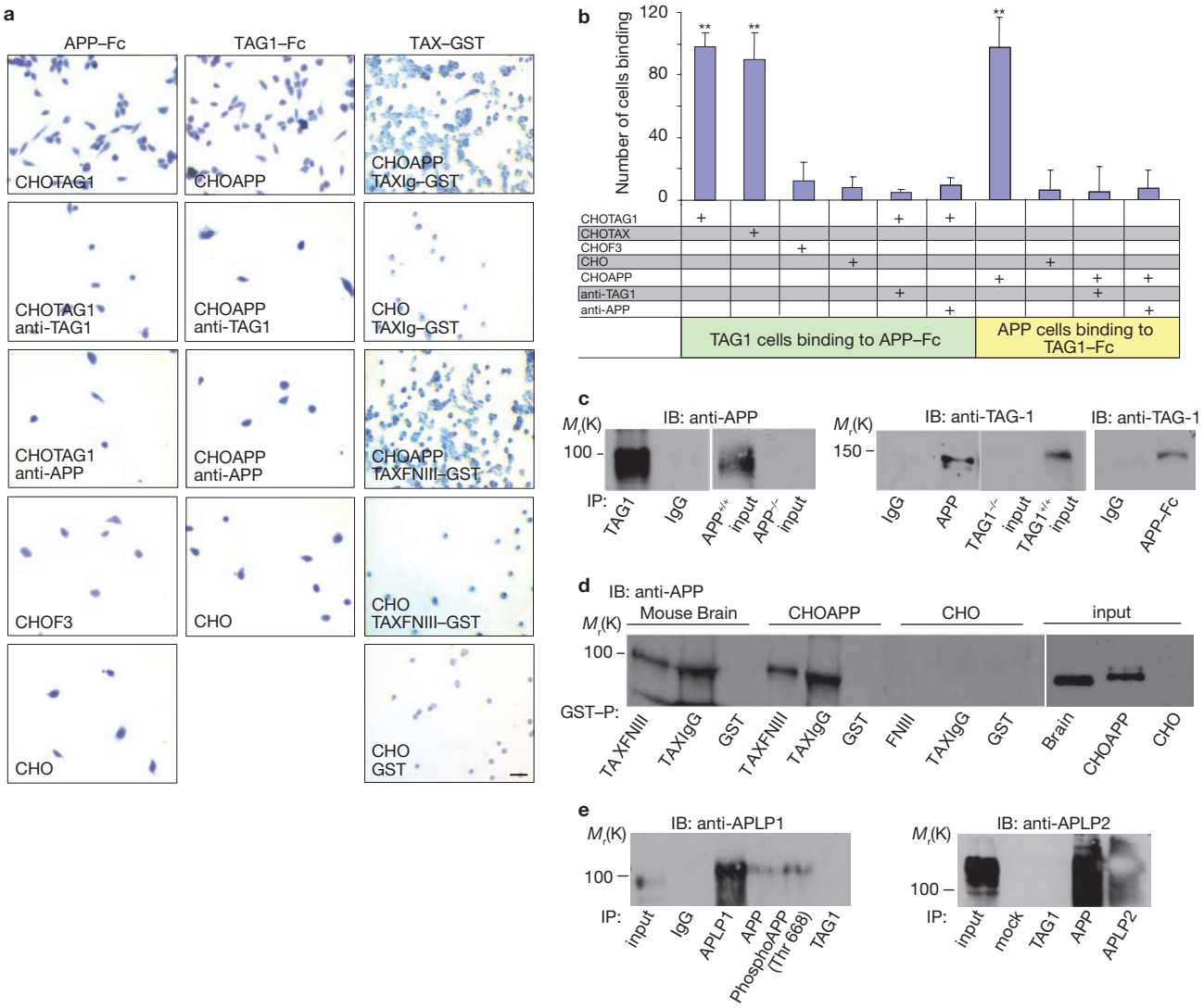

Figure 1 Cell adhesion assay showing that TAG1 is a binding partner of APP. (**a**) TAG1-transfected CHO (CHOTAG1) cells, but not F3-transfected (CHOF3) or non-transfected CHO (CHO) cells, adhered to APP–Fc protein spots. Adhesion of CHOTAG1 cells to APP–Fc was blocked by anti-TAG1 and anti-APP antibodies. APP-transfected CHO (CHOAPP) cells, but not CHO cells, adhered to spots coated with TAG1–Fc protein, TAXIg–GST and TAXFNIII–GST, but not GST. Adhesion of CHOAPP cells to TAG1–Fc was blocked by anti-TAG1 and anti-APP antibodies. Bar is 20 μm. (**b**) Quantification of CHOTAG1 cells adhering to APP–Fc substrate, CHOAPP adhering to TAG1–Fc substrate and the effects of blocking with anti-TAG1 and anti-APP antibodies (results shown as mean ± s.d., $n = 5–6$, $^{**}P < 0.001$). (**c**) Co-immunoprecipitation shows that APP and TAG1 associate as a protein complex. Brain lysates of wild-type mice were co-immunoprecipitated using an anti-TAG1 antibody (1C12) and non-immune IgG, and probed with an anti-APP antibody. Blotting of input from wild-type ($APP^{+/+}$) and *APP* knockouts ($APP^{-/-}$) confirmed the specificity of the antibody. Reciprocal assays used an anti-APP antibody (171610) or APP–Fc to capture the protein complex and anti-TAG1 antibodies to detect the binding partner. (**d**) GST Pull-down assay (GST–P) to analyse the interaction between TAX and APP. Mouse brain, CHOAPP and CHO cell lysates were precipitated using TAXFNIII–GST, TAXIg–GST and GST, and probed with an anti-APP antibody. Brain, CHOAPP and CHO inputs are shown in the right panel. (**e**) Brain lysates of wild-type mice were co-immunoprecipitated using antibodies against APLP1, APLP2, APP, phoshoAPP (Thr 668), TAG1 and non-immune IgG, and probed with antibodies against APLP1 and APLP2. Full scans of gels in **c**–**e** are shown in Supplementary Information, Fig. S6.

(Fig. 1a). Adhesion could be blocked by pre-treating the cells with an anti-TAG1 antibody or the culture dishes with an anti-APP antibody (22C11; Fig. 1a), indicating that the interaction of TAG1 with APP contributes to adhesion. In reciprocal adhesion assays, in which APP-transfected CHO (CHOAPP) cells were plated on culture dishes with TAG1–Fc protein spots, we observed similar adhesion of cells to the protein spots (Fig. 1a). Cell adhesion was blocked by neutralization of coated TAG1 protein spots or cell-membrane-bound APP with their respective antibodies (Fig. 1a, b). Likewise, control, non-transfected CHO cells did not adhere to the TAG1 protein spots (Fig. 1a, b). To identify the APP-binding domains in TAX, GST fusion proteins of the six immunoglobulin (Ig) domains (TAXIg–GST) and four fibronectin type III (FNIII) repeats (TAXFNIII–GST) of TAX were used as coated protein substrates for CHOAPP cells. The cells bound to spots of both proteins (Fig. 1a), indicating that APP has at least two binding sites located in the TAG1 Ig domains and FNIII repeats. Consistently, control, non-transfected CHO cells did not adhere to either of these two proteins or to GST alone (Fig. 1a).

© 2008 Nature Publishing Group

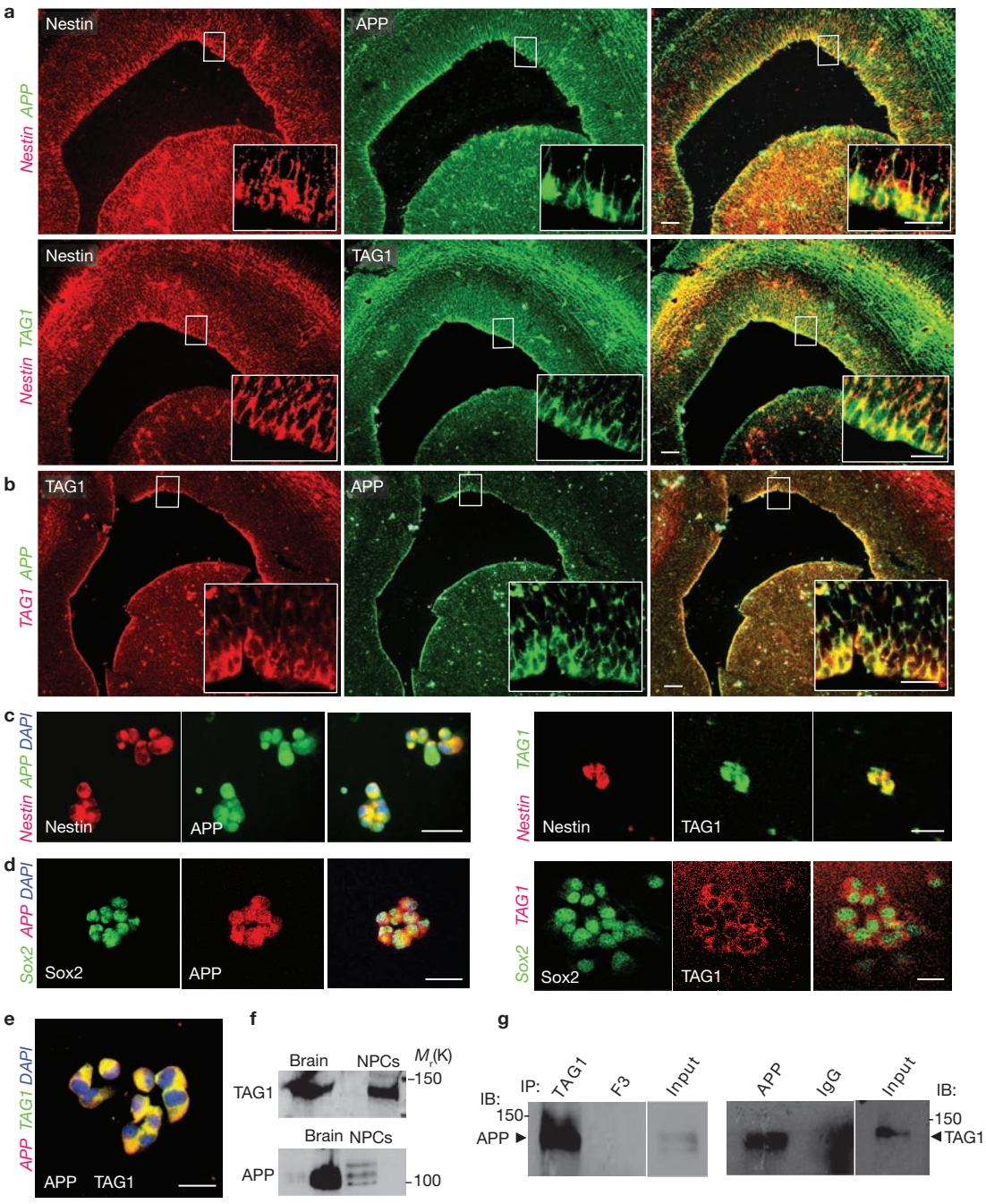

Figure 2 Expression of APP and TAG1 in the fetal neural stem cell niche and NPCs. (**a**) Double immunostaining for nestin (red) and APP (green) or TAG1 (green) in the walls of the lateral ventricles in E14 mouse brain. Bars are 50 μm (left) and 20 μm in higher magnification images (right). (**b**) Double immunostaining for APP (green) and TAG1 (red) in the walls of the lateral ventricles in E14 mouse brain. Bars are 50 μm (left) and 20 μm in higher magnification images (right). (**c**) NPCs isolated from the lateral ventricles of E14 mouse brain were double-stained for APP (green) or TAG1 (green) and neural precursor cell marker, nestin (red). Bars are 20 μm. (**d**) NPCs isolated from the lateral ventricles of E14 mouse brain were double-stained for APP (red) or TAG1 (red) and neural precursor cell marker, Sox2 (green). Bars are 20 μm. (**e**) NPCs isolated from the lateral ventricles of E14 mouse brain were double-stained for APP (red) and TAG1 (green). Bar is 20 μm. (**f**) Mouse brain samples and NPC lysates were analysed by western blotting with anti-TAG1 (TG1) and anti-APP (22C11) antibodies. (**g**) NPC lysates of wild-type mice were co-immunoprecipitated using anti-TAG1 (1C12) or anti-F3 antibodies and probed with an anti-APP antibody (22C11). Reciprocal assays used anti-APP antibody (171610) or non-immune IgG to capture the protein complex and an anti-TAG1 antibody (TG1) was used to detect the binding partner. Full scans of gels in **g** are shown in Supplementary Information, Fig. S6.

Next, we performed immunoprecipitation and Fc or GST pull-down assays in adult mouse brains to confirm that TAG1 interacts with APP. The results showed that several antibodies against TAG1, including 1C12 (Fig. 1c), 4D7 and TG3 (Supplementary Information, Fig. S1a), but not IgG or an anti-F3 antibody (Supplementary Information, Fig. S1a), could precipitate APP from wild-type mouse brains (Fig. 1c). Conversely, an anti-APP antibody (171610) could precipitate TAG1 from wild-type brains (Fig. 1c). Inputs (Fig. 1c) and immunoprecipitation controls

© 2008 Nature Publishing Group

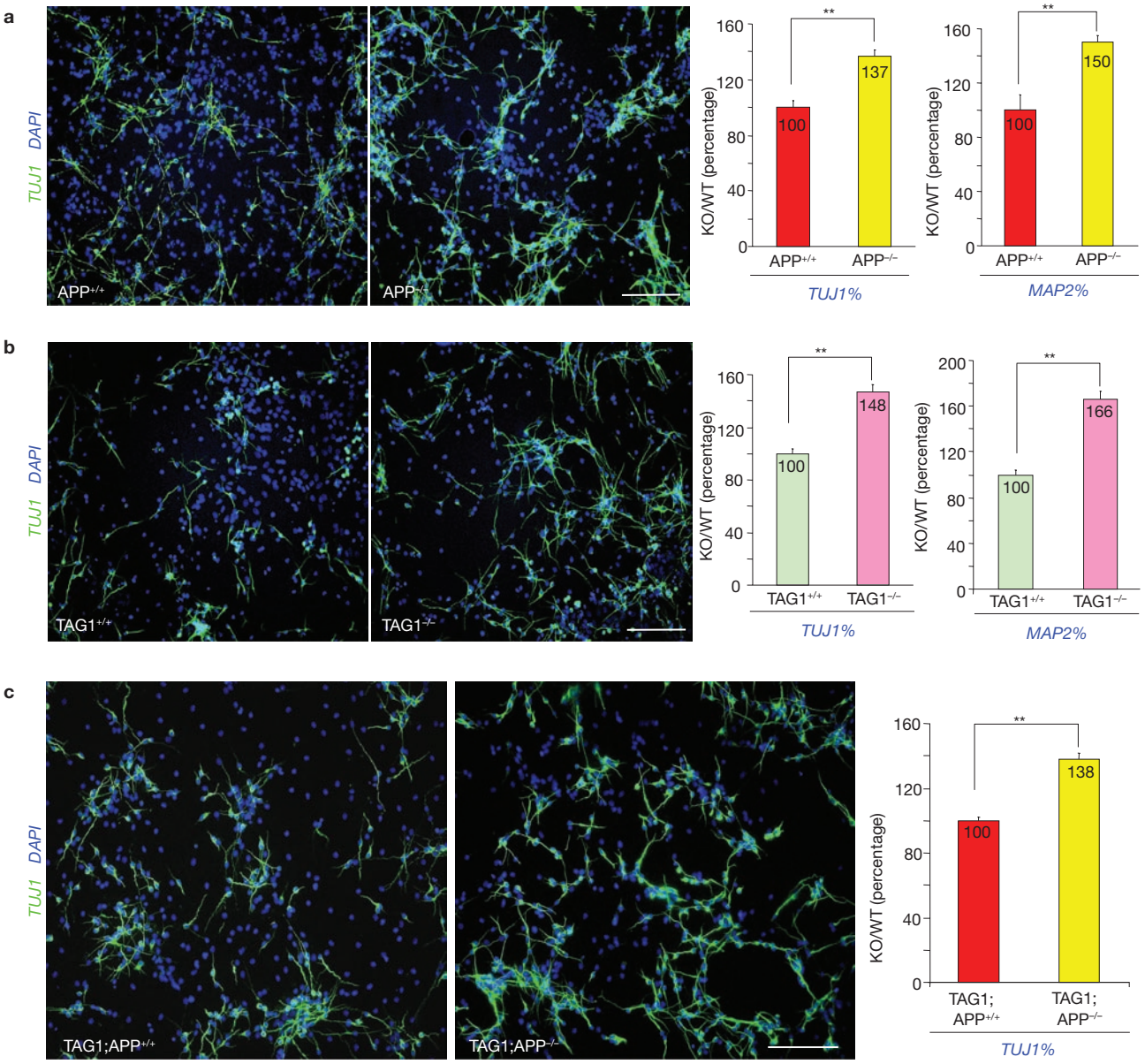

Figure 3 Neurogenesis in NPCs isolated from *APP*$^{+/+}$ and *APP*$^{-/-}$ (**a**), *TAG1*$^{+/+}$ and *TAG1*$^{-/-}$ (**b**), and *TAG1*$^{+/+}$;*APP*$^{+/+}$ and *TAG1*$^{-/-}$;*APP*$^{-/-}$ double mutant (**c**) mice. After 7–8 days *in vitro* culture differentiation, the cells were double-stained for TUJ1 or MAP2 and DAPI (shown in left panels). The numbers of TUJ1- and MAP2-positive cells were counted and expressed as a percentage of the number of DAPI-positive cells, normalized to the respective wild-type littermate controls (shown in the right panels) for APP (*APP*$^{-/-}$ TUJ1: 36.63 ± 1.12%; MAP2: 29.44 ± 1.04%; *APP*$^{+/+}$ TUJ1: 26.81 ± 1.36%; MAP2: 19.66 ± 2.20%; **a**), TAG1 (*TAG1*$^{-/-}$ TUJ1: 39.55 ± 1.34%; MAP2: 34.07 ± 1.50%; *TAG1*$^{+/+}$ TUJ1: 26.86 ± 0.90%; MAP2: 20.51 ± 0.82%; **b**) and TAG1;APP double mutants (*TAG1*$^{-/-}$;*APP*$^{-/-}$: 42.47 ± 1.05%; *TAG1*$^{+/+}$;*APP*$^{+/+}$: 30.73 ± 0.69%, **c**). Bars are 100 μm. Results are mean ± s.e.m., n = 3–6, $^{**}P < 0.001$.

(Supplementary Information, Fig. S1b, c) from the respective wild-type and knockout mouse brains confirmed the specificity of co-immunoprecipitation and the antibodies used. Consistent with the cell-adhesion results, APP–Fc precipitated TAG1 from mouse brains (Fig. 1c) and both TAXIg–GST and TAXFNIII–GST precipitated APP from mouse brains as well as from CHOAPP cells (Fig. 1d). In contrast to antibodies against APP, those directed against phosphoAPP (Thr 668), TAG1 (1C12), amyloid precursor-like protein 1 (APLP1) and APLP2 and could not precipitate APLP1 or APLP2 from wild-type mouse brains (Fig. 1e). These results demonstrate that APP and TAG1 bind to each other.

TAG1 and APP colocalize in the neurogenic ventricular zone and neural progenitor cells

We studied the localization of TAG1 and APP in embryonic day (E) 14 mouse brains by immunofluorescence labelling, using antibodies against TAG1 (AF1714) and APP (C7, Fig. 2a; 22C11, Fig. 2b). Immunofluorescence microscopy showed that APP or TAG1 were colocalized with nestin (Fig. 2a), a neural progenitor-cell marker, in the walls of the lateral ventricles of wild-type but neither in *APP*$^{-/-}$ nor *TAG1*$^{-/-}$ mice (Supplementary Information, Fig. S1d). Double immunofluorescence labelling showed that APP and TAG1 were co-expressed in the lateral ventricle

© 2008 Nature Publishing Group

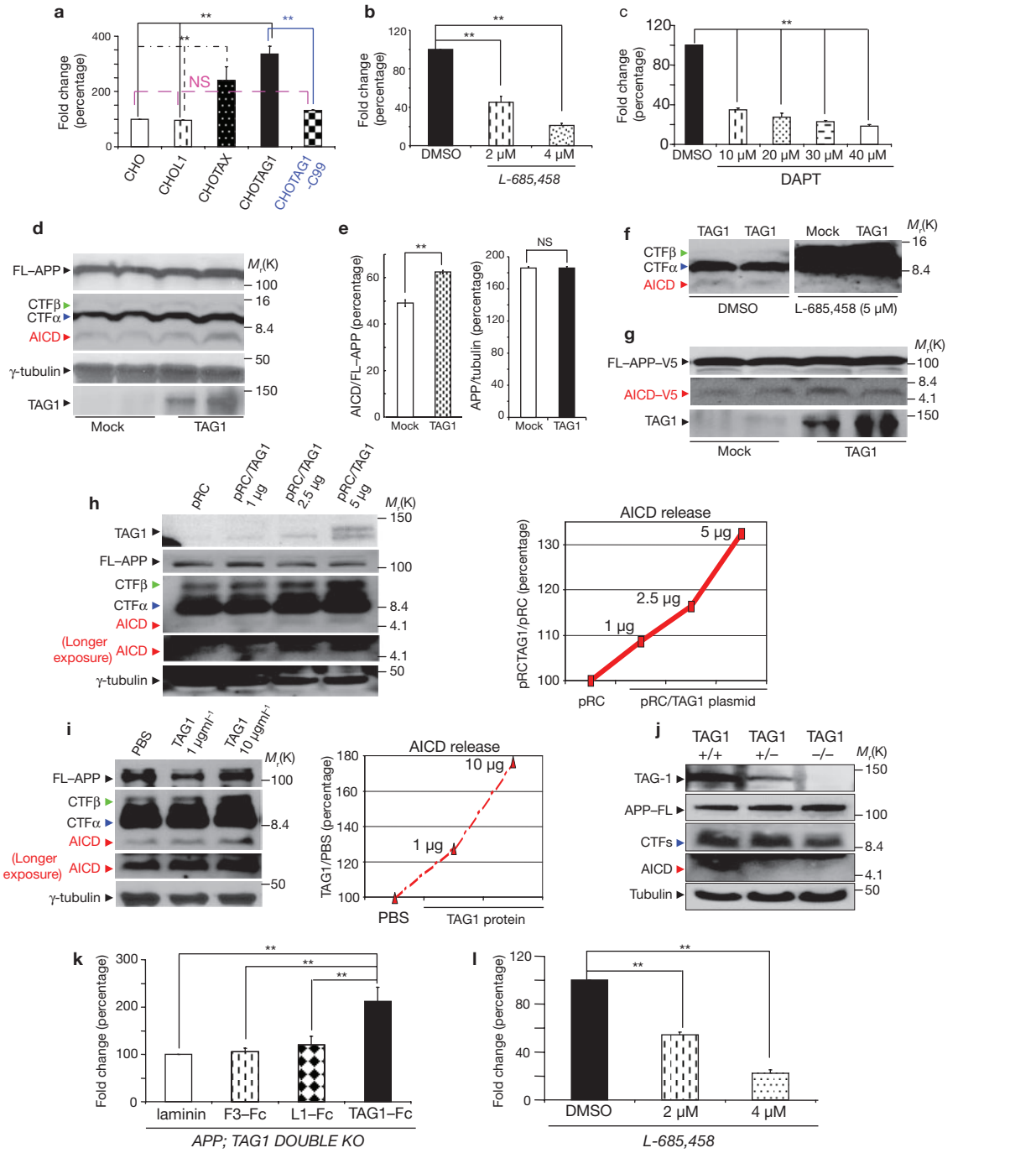

Figure 4 TAG1 triggers AICD release. (**a**–**c**) Luciferase assay for release of AICD–Gal4 in CHOTAG1 and CHOTAX cells. CHOL1, CHOTAX, CHOTAG1 and CHO cells were transiently co-transfected with pG5E1B plasmid, an APP–Gal4 construct or a C99–Gal4 construct, Fe65 plasmid, and luciferase internal control plasmid. Cleavage of APP to release AICD–Gal4 activates the luciferase reporter (**a**). Activity in CHOTAG1 cells was significantly reduced by two γ-secretase inhibitors, L-685,458 (**b**) and DAPT (**c**). (**d**, **e**) CHOAPP cells were co-transfected with cDNAs of Fe65, PS1 and TAG1 or pRC vector (Mock) as a control. Total protein obtained from the cells was analysed by western blotting using antibodies against C-terminal APP (A8717), TAG1 (TG1) and γ-tubulin (**d**). AICD and full-length APP (FL–APP) bands were quantified relative to FL–APP and γ-tubulin (**e**). (**f**) AICD release triggered by TAG1 in CHOAPP cells was significantly reduced by a γ-secretase inhibitor (L-685,458). (**g**) CHO cells were co-transfected with cDNAs of APP–V5, Fe65, BACE1 and TAG1 or pRC vector (Mock) as a control. Total proteins were analysed by western blotting using antibodies against C-terminal APP (A8717), TAG1 (TG1), V5 (R960-25) and γ-tubulin. (**h**–**j**) TAG1 and endogenous AICD production. Western blotting of total proteins was performed using antibodies against C-terminal APP (A8717), TAG1 (TG1) and γ-tubulin. MEFs were transfected with *TAG1* cDNA in pRC vector or empty pRC vector as a control (**h**). MEFs were treated for 3 h at 37 °C with PBS or TAG1 (**i**). E15 brain from *TAG1*$^{+/+}$, *TAG1*$^{+/-}$ and *TAG1*$^{-/-}$ mouse embryos (**j**). (**k**, **l**) TAG1-triggered release of AICD–Gal4 in NPCs from *TAG1;APP* double knockout mice. NPCs isolated from *TAG1*$^{-/-}$;*APP*$^{-/-}$ mice were transiently co-transfected with pG5E1B plasmid, an APP–Gal4 construct, Fe65 plasmid and luciferase internal control plasmid. Transfected NPCs were cultured in dishes substrate-coated with laminin, F3–Fc, L1–Fc or TAG1–Fc. Normalized luciferase activities in whole-cell lysates were determined and expressed relative to the activity in laminin-treated cells (**k**). TAG1-triggered luciferase activity in *TAG1*$^{-/-}$;*APP*$^{-/-}$ NPCs was significantly reduced by a γ-secretase inhibitor (L-685,458; **l**). Results are means ± s.e.m, $n = 3$–6, $^{**}P < 0.001$. Full scans of the gels shown in **d**, **f**–**j** are shown in Supplementary Information, Fig. S6.

© 2008 Nature Publishing Group

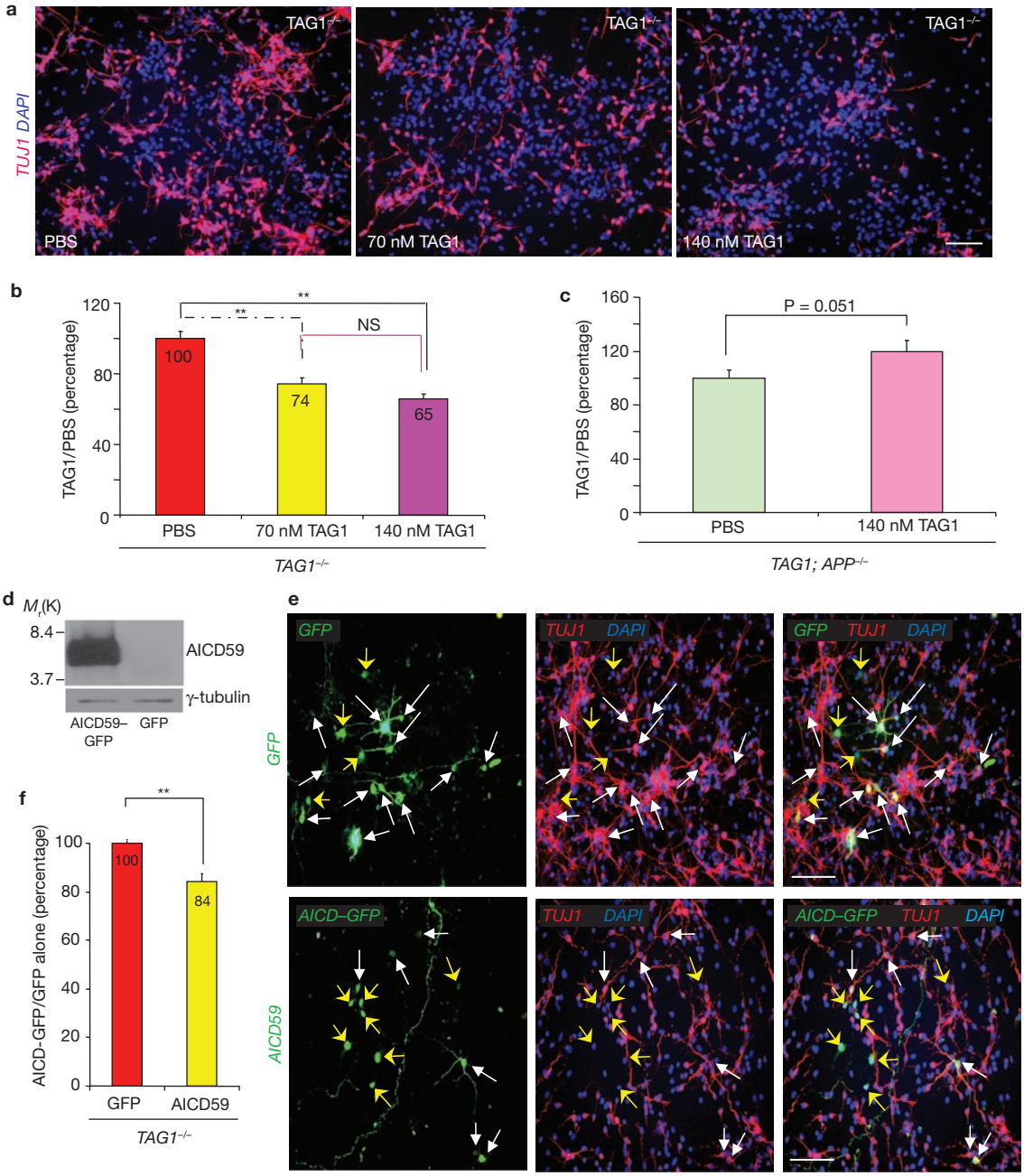

Figure 5 Neurogenesis in the NPCs of TAG1-deficient mice is reduced by treatment with either TAG1 or AICD. (**a**–**c**) NPCs were isolated from *TAG1*$^{-/-}$ (**a**, **b**) and *TAG1*$^{-/-}$;*APP*$^{-/-}$ (**c**) double-knockout mice and treated with TAG1 (70 nM and 140 nM) or PBS as a control. After differentiation, the cells were double-stained for TUJ1 and DAPI (**a**). The number of TUJ1- (**b**, **c**) positive cells was counted and expressed as a percentage of the number of DAPI-positive cells (*TAG1*$^{-/-}$ 70nM TAG1: 25.71 ± 1.27%; 140 nM TAG1: 22.69 ± 1.00%; *TAG1*$^{-/-}$;*APP*$^{-/-}$: 140 nM TAG1: 37.38 ± 2.52%), normalized to the respective PBS controls (*TAG1*$^{-/-}$ PBS: 34.65 ± 1.37%; *TAG1*$^{-/-}$;*APP*$^{-/-}$ PBS: 31.22 ± 1.90%). (**d**). Human *AICD59* cDNAs were cloned into the pCDF1–MCS1–EF1-copGFP mammalian expression vector. HEK293 cells in 60-mm plates were transfected with AICD59 or empty vector and harvested 24 h after transfection. The cell lysate was subjected to western blotting using antibodies against c-terminal APP and γ-tubulin. (**e**, **f**) NPCs were isolated from *TAG1*$^{-/-}$ and co-transfected with AICD59 and GFP in a pCDF1–MCS1–EF1–copGFP vector (AICD59) and empty vector containing only GFP (GFP) as a control. After differentiation, the cells were double-stained for TUJ1 and DAPI (**e**). White arrows indicate neurons infected with GFP or AICD59 and GFP and yellow arrows indicate non-neurons infected with GFP or AICD59 and GFP (**e**). The numbers of TUJ1-positive neurons infected with AICD59 and GFP (58.21 ± 2.21%) or GFP (69.06 ± 2.14%) were counted and normalized as a percentage of the total number of GFP-positive neurons (**f**). Bars are 100 μm. Results are mean ± s.e.m., $n = 5$, $^{**}P < 0.001$. Full scans of gels shown in **d** are shown in Supplementary Information, Fig. S6.

walls (Fig. 2b), indicating that these two molecules are colocalized in the neural stem-cell niche. Next, we isolated neural progenitor cells (NPCs) from E14 mouse telencephalic ventricular walls and double-stained them for APP (C7, green, Fig. 2c; MAB343, red, Fig. 2d) or TAG1 (TG1, green, Fig. 2c; 4D7, red, Fig. 2d) and the neural progenitor markers, nestin (red, Fig. 2c) or Sox2 (green, Fig. 2d). The results indicate that both APP and

© 2008 Nature Publishing Group

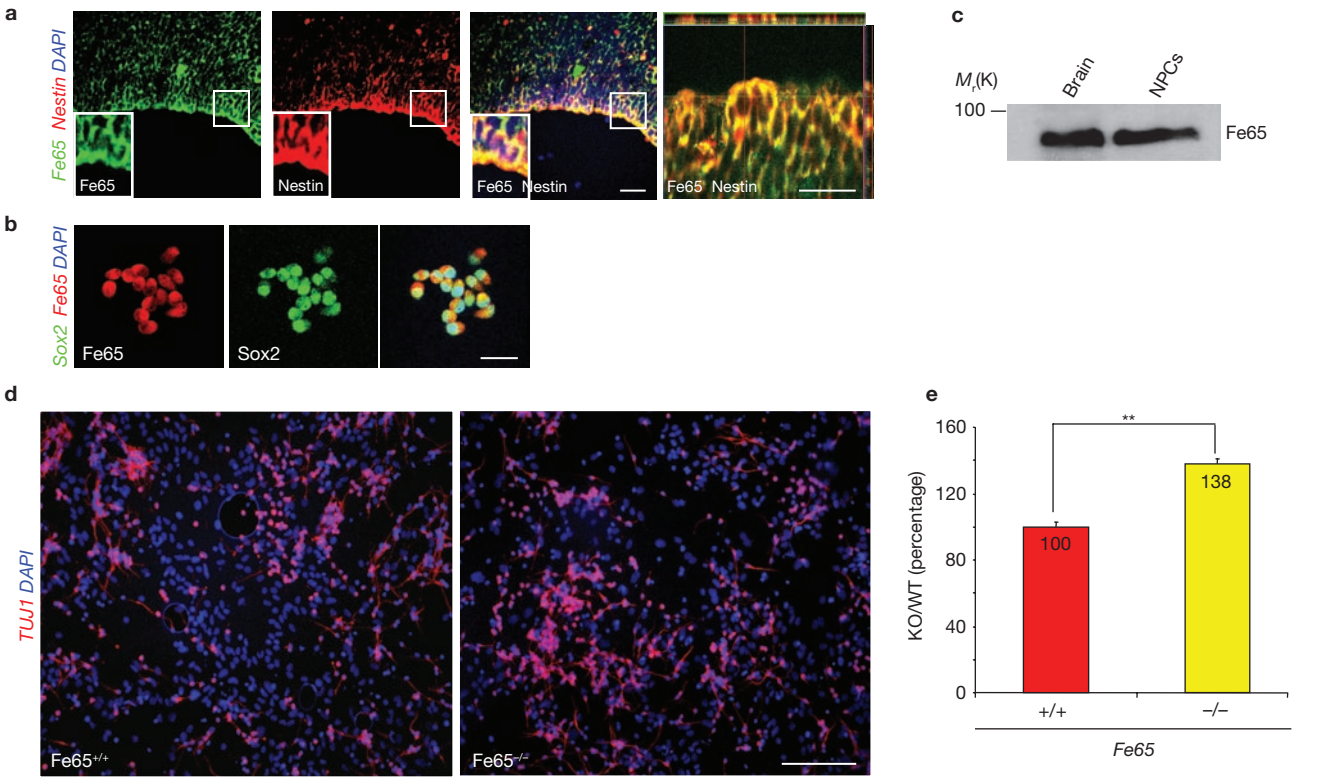

Figure 6 Expression of Fe65 in the fetal neural stem cell niche and NPCs and downregulated neurogenesis in NPCs isolated from Fe65-knockout mice. (**a**) Double immunostaining for nestin (red) and Fe65 (green) in the walls of the lateral ventricles in E14 mouse brain. (**b**) NPCs isolated from the lateral ventricles of E14 mouse brain were double-stained for Sox2 (green) and Fe65 (red). Scale bar is 20 μm. (**c**) Mouse brain samples and the NPC lysates were analysed by western blotting with antibodies against Fe65. (**d**, **e**) NPCs were isolated from *Fe65*$^{+/+}$ mice and *Fe65*$^{-/-}$ mice. After 7–8 days *in vitro* culture differentiation, the cells were double-stained for TUJ1 and DAPI (**d**). The number of TUJ1-positive neurons was counted and expressed as a percentage of the number of DAPI-positive cells (Fe65$^{-/-}$ 41.11 ± 0.95%) normalized to the respective wild-type littermate control (Fe65$^{+/+}$ 29.78 ± 0.87%; **e**). Results are mean ± s.e.m., $n = 3–5$, $^{**}P < 0.001$.

TAG1 are expressed by NPCs. Double-staining for APP (22C11) and TAG1 (TG3) also showed that these proteins are colocalized in NPCs (Fig. 2e). Consistent with these observations, western blotting with anti-TAG1 (TG1) and anti-APP (22C11) antibodies detected TAG1 and APP bands, respectively, in both mouse brain and NPCs (Fig. 2f). The interaction between TAG1 and APP was confirmed by immunoprecipitation in isolated NPCs using antibodies against APP (171610) and TAG1 (1C12) (Fig. 2g), suggesting that the interaction between these two molecules may also occur in NPCs. These results demonstrate that both TAG1 and APP are expressed by NPCs in the neural stem-cell niche.

TAG1 and APP modulate neurogenesis

To assess the role of the TAG1–APP interaction in modulating neurogenesis, NPCs were isolated from E14 telencephalic ventricular walls of *APP*$^{-/-}$ (Fig. 3a) and *TAG1*$^{-/-}$ (Fig. 3b) mice. *APP* null mice show increased mortality after birth. Adult *APP* null mice are usually smaller than wild-type mice but at E14 there are no observable gross phenotypic differences. *TAG1* null mice show no gross phenotypic abnormalities, although the adult mice exhibit elevated expression of adenosine A1 receptors in the hippocampus and increased seizure susceptibility to convulsant stimuli[6]. Seven to eight days after *in vitro* differentiation, cells were double-stained for class III β-tubulin (TUJ1, green; Fig. 3a, b) or microtubule-associated protein 2 (MAP2; data not shown), two markers of differentiated neurons, and DAPI (blue; Fig. 3a, b). Both TUJ1- and MAP2-positive cells were significantly increased in *APP*- and *TAG1*-knockout mice (Fig. 3a, b, respectively), compared with wild-type littermates. TUNEL assay showed that the number of apoptotic cells was not different between *TAG1*$^{-/-}$ and *TAG1*$^{+/+}$ NPC cultures (Supplementary Information, Fig. S2a). We also generated *TAG1*$^{-/-}$;*APP*$^{-/-}$ fetuses and found that this double knockout was usually developmentally lethal; few mice survived to birth but some fetuses were recovered at E14. Consistent with our observations in single knockout mice, TUJ1-positive cells were significantly increased in *TAG1*$^{-/-}$;*APP*$^{-/-}$ double-knockout mice, compared with wild-type littermates (Fig. 3c). These results demonstrate that the interaction between TAG1 and APP may be involved in modulating neurogenesis during the early stages of CNS development.

TAG1 stimulates AICD release

We investigated whether TAG1 could regulate AICD release in an artificial luciferase reporter system[7]. In this system, the Gal4 DNA-binding domain of *Saccharomyces cerevisiae* was inserted into the intracellular tail of full-length APP at the cytoplasmic boundary of the transmembrane region[7]. Only after γ-secretase cleavage is the AICD–Gal4 element released to drive luciferase reporter activity by means of the Gal4 response element. This system measures release of AICD but does not demonstrate that AICD is involved in endogenous transcriptional activation. We introduced this reporter system, together with Fe65, into non-transfected CHO and CHOL1, CHOTAG1 or CHOTAX cells. A

© 2008 Nature Publishing Group

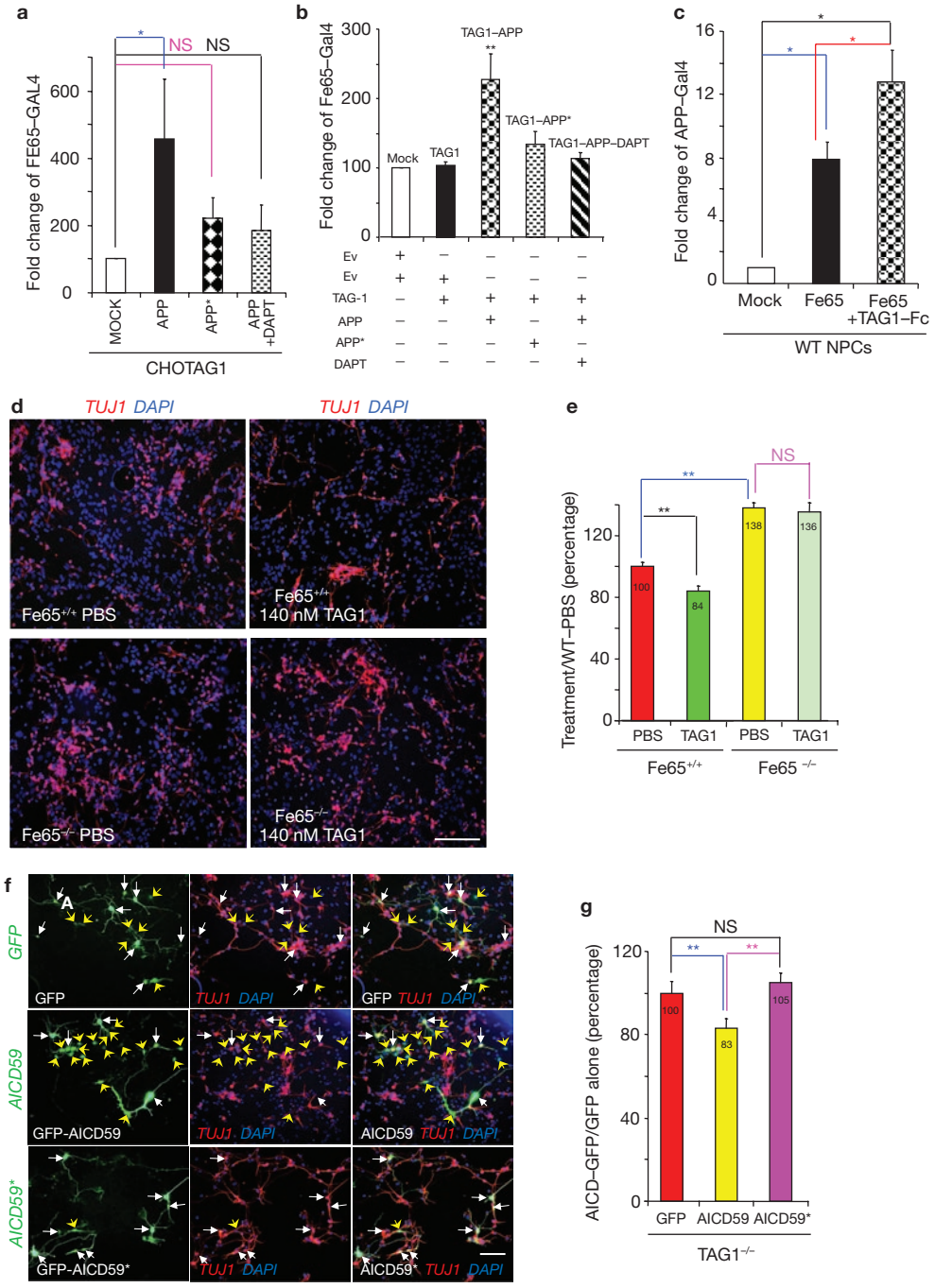

Figure 7 TAG1–APP signalling pathway through Fe65 modulates neurogenesis. (**a**–**c**) Fe65–Gal4 activity in CHOTAG1 cells transiently co-transfected with pG5E1B plasmid, Fe65–Gal4 construct, luciferase internal control plasmid, and *APP* cDNA or mutant *APP* (NPTY to NATA mutation; *APP**) as well as empty vector (Mock). A γ-secretase inhibitor (DAPT, 40 μM) significantly reduced luciferase activity (**a**). Activity of Fe65–Gal4 in CHO cells (**b**). CHO cells were transiently co-transfected with pG5E1B plasmid, Fe65–Gal4 construct, luciferase internal control plasmid, *TAG1* cDNA and *APP* cDNA or *APP** mutant as well as empty vector (Ev; Mock). DAPT (40 μM) significantly reduced luciferase activity. TAG1-triggered AICD release in wild-type NPCs (**c**). NPCs were transiently co-transfected with pG5E1B plasmid, APP–Gal4 construct, Fe65 plasmid, and luciferase internal control plasmid. The NPCs were cultured in dishes with or without TAG1 coating. Normalized luciferase activities in whole-cell lysates were expressed relative to activity in CHOTAG1 cells (**a**, **b**), CHO cells (**b**) or NPCs (**c**) with mock transfection. (**d**, **e**) NPCs were isolated from *Fe65*$^{+/+}$ and *Fe65*$^{-/-}$ mice and treated with TAG1 or PBS. After 7–8 days differentiation *in vitro*, cells were double-stained for TUJ1 and DAPI (**d**). TUJ1-positive cells were quantified relative to the number of DAPI-positive cells in the wild-type PBS control (**e**). (**f**, **g**) NPCs were isolated from TAG1$^{-/-}$mice and transfected with AICD and GFP with a pCDF1–MCS1–EF1–copGFP vector (AICD59), AICD mutant (NPTY to NATA mutation; AICD59*) or empty vector containing only GFP (GFP). After 7–8 days differentiation *in vitro*, cells were double-stained for TUJ1 and GFP (**f**). White arrows indicate neurons infected with GFP or AICD59 or AICD59* and GFP and yellow arrows indicate non-neurons infected with GFP or AICD59 or AICD59* and GFP. The numbers of GFP and TUJ1 double-positive neurons were counted and expressed as a percentage of the number of GFP-positive cells normalized to the respective GFP-only control (**g**). Results are means ± s.e.m. (**a**, **b**, **e**, **g**) or s.d. (**c**), n = 3–5, $^{*}P < 0.05$; $^{**}P < 0.001$.

© 2008 Nature Publishing Group

significant upregulation of the reporter activity was observed in both CHOTAG1 and CHOTAX cells but neither in the control nor CHOL1 cells (Fig. 4a; Supplementary Information, Fig. S3a–c). To confirm that the extracellular interaction between APP and TAG1 is essential for triggering AICD luciferase activity, we transfected a modified luciferase reporter system (C99), in which the extracellular domain of APP was deleted from the aforementioned APP–Gal4 construct, into CHOTAG1 cells (Supplementary Information, Fig. S3a). In these cells, reporter activity was no longer increased (Fig. 4a). Moreover, two specific γ-secretase inhibitors, L-685,458 and DAPT, reduced the TAG1-triggered release of AICD in a concentration-dependent manner (Fig. 4b, c). In contrast, TAG1 did not activate NICD-dependent, Hes1-mediated activity (Supplementary Information, Fig. S3d). These observations suggest that TAG1 triggers AICD release in a γ-secretase dependent manner.

To support the notion that TAG1 can trigger AICD release after binding with full-length APP, we investigated the AICD level by western blotting. CHOAPP cells were co-transfected with cDNAs of Fe65, presenilin-1 (PS1) and TAG1 or empty vector (plasmid pRC) as a control. Cell lysates were subjected to western blotting using antibodies against the C-terminal of APP (A8717), TAG1 (TG1) and γ-tubulin. Transfection with *TAG1* cDNA, but not the empty vector, significantly increased AICD release in the CHOAPP cells (Fig. 4d, e) and this increase was blocked by a γ-secretase inhibitor, L-685,458 (5 μM; Fig. 4f). The level of APP expression was not different between these two groups (Fig. 4e). CHO cells were also co-transfected with cDNAs of APP–V5 (APP fused with the V5 epitope tag sequence derived from the P and V proteins of Simian virus 5), Fe65, BACE1 and TAG1 or pRC vector (Mock) as a control and total protein was analysed by western blotting with antibodies against TAG1 (TG1), V5 (R960-25) and γ-tubulin (Fig. 4g). Western blotting with an anti-V5 antibody showed that TAG1 transfection increased AICD–V5 release in CHO cells compared with the mock transfection control (Fig. 4g).

To ascertain whether TAG1 could also stimulate endogenous release of AICD, we transfected mouse embryonic fibroblasts (MEFs) with an empty pRC vector or with various concentrations of *TAG1* cDNA. We observed a concentration-dependent increase in the production of endogenous AICD (Fig. 4h). We also compared the effects of two concentrations of TAG1 protein on endogenous AICD production in MEFs. Again there was a concentration-dependent increase in the production of endogenous AICD in cells treated with TAG1 (Fig. 4i). The effect of TAG1 on endogenous AICD production was further confirmed by investigation of AICD expression in E15 brains of $TAG1^{+/+}$, $TAG1^{+/-}$ and $TAG1^{-/-}$ mouse embryos. There was a reduction in expression of endogenous AICD in the heterozygous and homozygous *TAG1*-null mouse brains that corresponded with the reduction in expression of TAG1 (Fig. 4j). However, there was no change in NICD and Hes protein expression in TAG1-null mouse brains (Supplementary Information, Fig. S3e). In addition to AICD production, which requires γ-secretase cleavage, C-terminal fragment- (CTF) α and CTF-β were detected in the *in vitro* cell culture experiments. There was a marked preponderance of CTF-α over CTF-β but both CTF-α and CTF-β increased in response to TAG1 (Fig. 4d, h, i), suggesting that, although α-secretase cleavage dominates, both α- and β-secretase cleavage increase in response to TAG1.

To further examine the notion that TAG1 is a functional ligand of APP, capable of triggering the release of AICD, we used the luciferase reporter system in cells isolated from $TAG1^{-/-};APP^{-/-}$ embryos to investigate whether TAG1–APP interaction could modulate AICD release in fetal NPCs. After transfection with the APP luciferase reporter system, $TAG1^{-/-};APP^{-/-}$ NPCs were cultured as monolayers in culture dishes co-coated with TAG1–Fc, L1–Fc, F3–Fc or laminin. As expected, TAG1–Fc, but not F3–Fc, L1–Fc or laminin, strongly triggered reporter activity (Fig. 4k), indicating that AICD had been released. A specific γ-secretase inhibitor (L-685,458) blocked the induction of AICD release by TAG1 in a concentration-dependent manner (Fig. 4l), indicating that γ-secretase is involved in the TAG1 triggered RIP process in the $TAG1^{-/-};APP^{-/-}$ double knockout fetal NPCs. Similarly to the observations in CHOTAG1 and CHOTAX cells (Fig. 4a), these experiments demonstrate that AICD-dependent activity in the luciferase reporter system is also regulated by the interaction between TAG1 and APP in NPCs. Together, these results indicate that TAG1 may trigger AICD release by a γ-secretase-dependent mechanism.

AICD is necessary for the negative modulation of neurogenesis by the TAG1–APP signalling pathway

To investigate the role of the TAG1–APP signalling pathway in neurogenesis, we treated $TAG1^{-/-}$ and $TAG1^{-/-};APP^{-/-}$ fetal NPCs with soluble TAG1 (70 nM and 140 nM) during differentiation. The cells were double-stained for TUJ1 and DAPI and the amount of staining was quantified. After TAG1 treatment, the number of TUJ1-positive cells was significantly decreased in fetal NPCs from *TAG1*-null mice, compared with the PBS-treated control group (Fig. 5a, b, c). Similar treatment could not reverse the abnormally increased neurogenesis in $TAG1^{-/-};APP^{-/-}$ double knockout mice (Fig. 5c). Together these findings indicate that APP is a functional receptor of TAG1 that modulates neurogenesis. To test this idea, we transfected $TAG1^{-/-}$ knockout fetal NPCs with AICD59, an intracellularly active fragment of APP released after TAG1–APP interaction, together with green fluorescent protein (GFP) in the same vector but under the control of a different promoter (Fig. 5d, e). The number of TUJ1-positive cells in the AICD59 transfected group was significantly decreased, compared with the control group transfected with GFP alone (Fig. 5f; $P < 0.001$). Treatment with a γ-secretase inhibitor increased neurogenesis in wild-type NPCs (Supplementary Information, Fig. S4a; $P < 0.001$); however, a similar, but slightly less significant, effect was also observed in NPCs from *APP*-null mice (Supplementary Information, Fig. S4b; $P < 0.05$). To investigate whether AICD could induce apoptosis, we performed a TUNEL assay on the $TAG1^{-/-}$ NPCs transfected with either AICD59 or empty vector (GFP) as a control. There was no difference in the number of apoptotic cells between these two group cells (Supplementary Information, Fig. S2b), suggesting that AICD does not induce apoptosis in the transfected NPCs. These observations support the hypothesis that the TAG1–APP signalling pathway negatively regulates neurogenesis through AICD during early CNS development.

Fe65 is also expressed in the neurogenic ventricular zone and NPCs and negatively modulates neurogenesis

The mammalian Fe65 protein family consists of Fe65, Fe65L1 and Fe65L2. This class of scaffolding proteins has three structural domains, which include a WW domain (two tryptophans) and two phosphotyrosine-binding domains (PID1–PTB1 and PID2–PTB2) that mediate protein–protein interactions. All Fe65 protein family members bind to members of the APP protein family (APP, APLP1 and APLP2) through the C-terminal PID2–PTB2 domain[8]. It has been suggested that Fe65

© 2008 Nature Publishing Group

has a role in AICD-dependent transcriptional activation[7], but, unlike Fe65, the Fe65L1 and Fe65L2 interactions with APP do not activate APP-dependent transcription[9,10]. Therefore, we investigated whether Fe65 acts as a downstream element in the TAG1–APP signalling pathway regulating neurogenesis. We studied the localization of Fe65 expression in E14 mouse brains and in isolated NPCs from E14 mouse telencephalic ventricular walls by double immunofluorescence labelling, using antibodies against Fe65 and either nestin or Sox2. In the E14 mouse brain, immunofluorescence microscopy showed that Fe65 was colocalized with nestin (Fig. 6a) in the ventricular walls. Similarly, Fe65 colocalized with Sox2 in NPCs (Fig. 6b). Western blotting detected a Fe65 band in both NPCs and total mouse brain (Fig. 6c). These results demonstrate that Fe65, like TAG1 and APP, is expressed by NPCs in the neural stem-cell niche. To determine the developmental expression of TAG1, APP and Fe65, fetal brain lysates from E10 to postnatal day (P) 0 mouse brains were analysed by western blotting with antibodies against TAG1 (TG1), APP (A8717), Fe65 (3H6) and γ-tubulin (Supplementary Information, Fig. S5). TAG1 and Fe65 were present from E12, whereas APP was detectable from E10. TAG1 was most strongly expressed from E16 to E18, but APP and Fe65 levels continued to increase to P0. Thus, all three proteins are present during fetal brain development, with APP switching on as cortical neurogenesis peaks at E14 to E15 (ref. 11) and TAG1 peaking as cortical neurogenesis declines from E16 to E18 (ref. 11). Both APP and Fe65 then continue to increase to P0, whereas neurogenesis remains low. Next, we investigated neurogenesis in NPCs from *Fe65*$^{-/-}$ mice. Interestingly, the number of TUJ1-positive cells was significantly increased in NPCs from *Fe65*$^{-/-}$ mice, compared with NPCs from *Fe65*$^{+/+}$ mice (Fig. 6d, e). TUNEL assay showed that the number of apoptotic cells was not different between *Fe65*$^{-/-}$ and *Fe65*$^{+/+}$ NPC cultures (Supplementary Information, Fig. S2c). Thus, similarly to *TAG1*$^{-/-}$, *APP*$^{-/-}$ and *TAG1*$^{-/-}$;*APP*$^{-/-}$ mice, Fe65 deletion also leads to abnormal enhancement of neurogenesis.

Fe65 is a downstream element of TAG1–APP signalling during modulation of neurogenesis

Our observations imply that Fe65 may act as a downstream element in the TAG1–APP signalling pathway. To test this hypothesis, we introduced a luciferase reporter system in which Gal4 is fused to the N-terminal of Fe65 (ref. 12) into CHOTAG1 cells. When co-transfected with APP, but not with the empty vector used as a control, a significant upregulation of reporter activity was observed in CHOTAG1 cells (Fig. 7a). Notably, co-transfection with an APP mutant (APP*) that abolishes Fe65 binding and transactivation (NPTY to NATA mutation[12]) did not increase the TAG1-triggered, Fe65-dependent transcriptional activity (Fig. 7a); however, this activity was reduced by a specific γ-secretase inhibitor, DAPT (Fig. 7a). We introduced this luciferase reporter system into CHO cells. When *TAG1* cDNA, but neither TAG1 alone nor the empty vector control, was co-transfected with *APP* cDNA, but not the *APP** mutant, a significant upregulation of reporter activity was observed, which could be reduced by DAPT (Fig. 7b). To investigate whether both Fe65 and TAG1 could modulate intracellular release of AICD in wild-type fetal NPCs, these cells were transfected with the APP–Gal4 luciferase reporter system and Fe65, and were cultured as monolayers in culture dishes co-coated with TAG1–Fc and laminin. As expected, Fe65 increased the AICD-dependent reporter activity in the APP–Gal4-, Fe65-transfected NPCs, compared with those transfected with mock control or empty vector (Fig. 7c). Consistently, after TAG1–Fc treatment, the AICD-dependent reporter activity was markedly increased in the Fe65-transfected NPCs, compared with the non-treated group (Fig. 7c). Thus, these results demonstrate that TAG1 regulates not only AICD-dependent, but also Fe65-dependent, activity in the luciferase reporter system in a γ-secretase dependent manner, suggesting that TAG1 stimulation of APP causes intracellular release of AICD and activation of Fe65.

Next, we investigated whether TAG1 could modulate neurogenesis in fetal NPCs isolated from *Fe65*$^{-/-}$ mice. TAG1 protein was applied to trigger the TAG1–APP signalling pathway in fetal NPCs isolated from either *Fe65*$^{+/+}$ or *Fe65*$^{-/-}$ mice. The number of TUJ1-positive cells was significantly decreased in the TAG1-treated NPCs from *Fe65*$^{+/+}$ mice, compared with the PBS-treated group (Fig. 7d, e). However, TAG1 could not reverse the abnormal increase in neurogenesis in the *Fe65*$^{-/-}$ mice (Fig. 7d, e). To confirm that Fe65 has a role in the TAG1–APP-dependent modulation of neurogenesis, we transfected an AICD59 mutant (AICD59* that has a NPTY to NATA mutation[12]), into *TAG1*$^{-/-}$ NPCs. In contrast to AICD59, AICD59* could not reverse the abnormal enhancement of neurogenesis in *TAG1*$^{-/-}$ NPCs (Fig. 7f, g). Together, the observations that the abnormal enhancement of neurogenesis in the *TAG1*$^{-/-}$ NPCs can be reversed either by application of TAG1 (Fig. 5a) or transfection with AICD59 (Fig. 7f, g), and that AICD59* abolishes Fe65 binding and transactivation[12], support the notion that Fe65 acts as a downstream element in the TAG1–APP signalling pathway, which negatively regulates neurogenesis.

DISCUSSION

Using several approaches, including cell adhesion and co-immunoprecipitation, we have shown that TAG1, a member of the F3 family, binds to APP. TAG1 and APP colocalize in the neurogenic niche of the ventricular zone in the developing mouse brain. Similarly to F3-induced NICD activity[4], TAG1, as a functional ligand of APP, promotes AICD release in a γ-secretase-dependent manner. We showed that endogenous AICD production increases in a concentration-dependent manner in MEFs that have either been transfected with or treated with TAG1, whereas endogenous AICD production is reduced in embryonic *TAG1*-null mouse brains when compared with wild-type mice. Concentration-dependent increases in CTF-α and CTF-β in response to TAG1 were also observed *in vitro*. The increase in neurogenesis seen in neural stem cells isolated from *TAG1*-null mice was reversed by expression of AICD, confirming that negative modulation of neurogenesis is a physiological function of cleaved AICD. We further demonstrated that the TAG1–APP signalling pathway through Fe65 negatively modulates neurogenesis. These findings are important in the context of Alzheimer's disease as abnormal processing of APP may also lead to aberrant AICD generation, which may be linked to abnormal intracellular signalling. Further research is required to understand the details of the mechanisms by which the TAG1–APP signalling pathway, as well as its downstream elements, modulate neural stem cells. Knowledge of these mechanisms may provide insights into the cellular processes of neurodegenerative disease and may also offer unique opportunities for pharmacological intervention. □

METHOD

Antibodies. The following antibodies were used: anti-APP (C7 from D. J Selkoe, Harvard Medical School, Boston, MA); monoclonal anti-TAG1 (4D7 and 1C12 from A, J, Furley, University of Sheffield, UK); polyclonal anti-TAG1

© 2008 Nature Publishing Group

(TG3 (ref. 13); TG1 from K. Watanabe, Nagaoka University of Technology, Japan; AF1714, R&D Systems); anti-Fe65 (3H6, Upstate); anti-APLP1, -APLP2, -APP (22C11; MAB343; A4), and -MAP2 (Chemicon); rabbit anti-APP C-terminal (A8717, Sigma-Aldrich), goat anti-APP (171610, Calbiochem); anti-V5 (R960-25, Invitrogen); anti-Gal4 (Clontech); anti-Notch1 N1ICD (ab8925), anti-Notch2 N2ICD (ab28926) and anti-Hes5 (ab25374, Abcam); anti-Hes1 (AB5702, Chemicon); anti-nestin, -Sox2 and -GFAP (Dako); anti-β tubulinIII (TUJ1; Sigma-Aldrich); anti-γ-tubulin (Sigma-Aldrich); and anti-Myc (Santa Cruz Biotechnology).

Fc and GST fusion proteins. Mouse *APP 695* cDNA (from S. Sisodia, University of Chicago, IL) was subcloned into the pblue Bac vector to generate a fusion protein containing the extracellular domain of APP with the Fc part of human immunoglobulin G at its COOH-terminal end (APP–Fc). For details see the Supplementary Information. CHO K1 cells were stably transfected with the vector according to published procedures[14].

A soluble form of TAG1–Fc recombinant protein was produced in 293T cells. The signal sequence of the GPI-anchor of mouse TAG1 was substituted with human IgG–Fc followed by a termination codon. The recombinant cDNA was inserted at the *Hind*III–*Not*I sites of pDX, a modified pcDNA3 vector with an amplification-promoting sequence (APS)[15] upstream of the CMV site. The vector was introduced into 293T cells. Fc proteins were purified with the Fc-tag using Protein-A column chromatography, as has been described previously[14].

The sequences for the Ig and FNIII domains of TAG1 were inserted into the pGEX–KG vector to produce the GST-tagged fusion proteins. The recombinant vectors were introduced into the TOP10 strain of *Escherichia coli*, which was subsequently induced by IPTG (Bio-Rad Laboratories). The recombinant GST fusion proteins were purified using GST beads (Sigma-Aldrich), according to the manufacturer's instructions.

Cell adhesion assay. CHO cells stably transfected with mouse *APP 695* or transiently transfected with *APP*, *F3*, *TAX*, *TAG1* or mock cDNA, were cultured in DMEM containing 10% fetal calf serum. The cells were plated on dishes coated with methanol-solubilized nitrocellulose and then with proteins (12 μM). Blockade of adhesion was carried out using polyclonal anti-TAG1 (1:100) or anti-APP (1:100) antibodies. See the Supplementary Information for details. Cells adhering to the various protein spots were photographed and counted. The results were analysed by Newman-Keuls test with $P < 0.05$ considered significant.

GST or Fc pull-down assays. Freshly prepared cerebral hemispheres of adult rats were harvested and solubilized in 2% Triton X-100. The buffer homogenate was centrifuged at 13,000*g* for 1 h at 4 °C and the supernatant was incubated for 45 min at room temperature with glutathione-agarose or protein A-coupled agarose beads that had been incubated with TAG1–Fc or APP–Fc. After washing the beads, proteins were eluted with SDS–PAGE sample buffer and immunoblotted with anti-APP or anti-TAG1 antibodies.

Co-immunoprecipitation. Mouse brains and NPCs were lysed with RIPA buffer containing a protease inhibitor cocktail (Roche). For immunoprecipitation, lysates were precleared with protein A-coupled agarose beads for 1 h and incubated with APP or TAG1 antibodies together with protein A-coupled agarose overnight at 4 °C. Samples were washed with washing buffer before the beads were re-suspended in SDS buffer and boiled for 3–5 min. Samples were subjected to SDS–PAGE. Western blot analysis was performed and developed with ECL reagents (Amersham Biosciences).

Immunocytochemistry and quantification. Immunostaining of cultured cells and tissue sections was performed as described previously[15]. Photomicrographs were taken and cells were counted systematically. Each experiment was repeated on 3–7 mice. For details of quantification of immunofluorescence microscopy, see the Supplementary Information.

Deficient mice. *APP*$^{-/-}$ (ref. 16), *TAG1*$^{-/-}$ (ref. 6) and *Fe65*$^{-/-}$ (ref. 17) mice have been described previously. *TAG1;APP* double-deficient mice were generated by intercrossing APP homozygous and TAG1 homozygous (*APP*$^{-/-}$ X *TAG1*$^{-/-}$) mice. Animals heterozygous for both loci were intercrossed with each other (*TAG1*$^{+/-}$;*APP*$^{+/-}$ X *TAG1*$^{+/-}$;*APP*$^{+/-}$) to generate APP and TAG1 double-deficient (*TAG1*$^{-/-}$;*APP*$^{-/-}$) offspring.

Culture of neural progenitor cells. Telencephalic lateral ventricle walls isolated from E14 embryos were dissociated and neurosphere-forming cells were cultured in DMEM-F12 (Gibco) containing N2 supplement, 20 ng ml^{-1} bFGF and 20 ng ml^{-1} EGF. For differentiation assay, second passage neurospheres were collected and dissociated into single cells. The cell suspension was seeded into 24-well dishes with 20,000 cells per well and was induced in DMEM-F12 culture medium containing N2 and 0.5% fetal calf serum for 7–8 days. Nucleofeto II (Amaxa Biosystems) was used for plasmid transfection into NPCs.

TUNEL assay. TUNEL assay was performed according to the manufacturer's protocol (Chemicon).

Luciferase assay. The APP–Gal4 assay system has been described previously[7]. CHOL1, CHOTAG1, CHOTAX and non-transfected CHO cells were co-transfected with (1) pG5E1B-luc (Gal4 reporter plasmid); (2) pCMV–LacZ (β-galactosidase control plasmid); (3) pMstAPP (Gal4) or pMstC99 (Gal4); and (4) pCMV5–Fe65 (Fe65) in 24-well dishes. Cells likewise cultured in 24-well dishes were used for AICD–Gal4, C99–Gal4, APP*–Gal4 (with NPTY to NATA mutation), AICD59*–Gal4 (with NPTY to NATA mutation) and Fe65–Gal4 luciferase reporter assays. For the transactivation assay in NPCs, wells were coated with L1–Fc, TAG1–Fc, F3–Fc or laminin protein (8 nM). To examine the role of γ–secretase in this transactivation, different concentrations of γ–secretase inhibitors (L-685,458: 2 or 4 μM; DAPT: 10, 20, 30 or 40 μM; Calbiochem) were applied. Cells were lysed at 24 h after transfection and assayed using the Steady-Glo Luciferase Assay Kit (Promega). The Hes1 luciferase reporter assay has been described previously [4]. See the Supplementary Information for details.

Western blotting for AICD detection in CHO and MEFs, and E15 mouse brain. Protein extraction for detection of AICD in cell lines was performed as described previously[18,19]. The protein was loaded onto 16% SDS-Tricine polyacrylamide gel and transferred onto PVDF membranes. Protein extraction to detect AICD in mouse brain was performed as described previously[20]. The protein was applied to 12% SDS-Tricine polyacrylamide gels and transferred onto PVDF membranes. The PVDF membranes were processed for incubation with primary antibodies against the C-terminal of APP (A8717), TAG1 (TG1) and γ-tubulin and detection with ECL Plus or ECL Advance Western Blotting Detection Reagents (Amersham Biosciences). See the Supplementary Information for details.

Cloning of AICD59 and C99. The fragment of AICDC59 was obtained by PCR amplification of the indicated coding sequence of human *APP* cDNA using the primers: 5′-GGCGTCTAGAGCCACC ATGATAGCGACAGTGATCGTCAT CACC-3(and 5′-GGCGGCGGCCGCCTA GTTCTGCATCTGCTCAAAGA-3. The initial methionine (underlined) was artificially introduced. The product was digested with *Xba*I and *Not*I and subcloned into the *Xba*I–*Not*I site of pCDF1–MCS1–EF1–copGFP (System Biosciences). The construct was confirmed by sequencing and western blotting (Fig. 5d). The fragment of Gal4–C99 was obtained by PCR amplification from plasmid pMstAPP (Gal4) using the primers: 5′-GCGC TCTAGA GCCACC ATGGATGCAGAATTCCGACATG -3′ and 5′-GGCGGCGGCCGCCTA GTTCTGCATCTGCTCAAAGA-3. The product was digested with *Xba*I and *Not*I and subcloned into the *Xba*I–*Not*I site of pCDF–MCS1–EF1–copGFP. The construct was confirmed by sequencing.

Note: Supplementary Information is available on the Nature Cell Biology website.

ACKNOWLEDGEMENTS

We thank D. J. Selkoe for providing APP antibodies, T. Sudhof for the APP–Gal4, APP*–Gal4 and Fe65–Gal plasmids, S. Sisodia for mouse *APP 695* cDNA, C. Schmidt for APP–Fc, and Q. D. Hu, X. Y. Cui, J. L. Hu, F. C. K. Tan and S. Hébert for technical assistance. This work was supported by grants to Z. C. Xiao from the National Medical Research Council of Singapore, Singapore Health Services, Department of Clinical Research, Singapore General Hospital, Institute of Molecular and Cell Biology, A*STAR, Singapore, and a grant to both Z. C. Xiao and D. Bagnard from MERLION, a Singapore-France joint scientific programme. M. Schachner is New Jersey Professor for Spinal Cord Research

AUTHOR CONTRIBUTIONS

Q.-H. M, T. F., W.-L. Y. and L. Z. performed the experiments and analysed the data (the contribution of Q.-H. M. to the experimental work was greatest, whereas that of T. F., W.-L. Y. were equivalent); X.-D. J., Y. T., R.-X. X., D. B., M. S., A. J. F., D. K. and K. W. provided materials and input to the experimental design; G. S. D. and Z.-C. X. planned and directed the project, designed the experiments and wrote the manuscript.

© 2008 Nature Publishing Group

Published online at http://www.nature.com/naturecellbiology/
Reprints and permissions information is available online at http://npg.nature.com/reprintsandpermissions/

1. Parks, A. L. & Curtis, D. Presenilin diversifies its portfolio. *Trends Genet.* **23,** 140–150 (2007).
2. Karagogeos, D. Neural GPI-anchored cell adhesion molecules. *Front. Biosci.* **8**, s1304-s1320 (2003).
3. Cui, X. Y. *et al.* NB-3/Notch1 pathway via Deltex1 promotes neural progenitor cell differentiation into oligodendrocytes. *J. Biol. Chem.* **279,** 25858–25865 (2004).
4. Hu, Q. D. *et al.* F3 acts as a functional ligand for Notch during oligodendrocyte maturation. *Cell* **115,** 163–175 (2003).
5. Selkoe, D. & Kopan, R. Notch and Presenilin: regulated intramembrane proteolysis links development and degeneration. *Annu. Rev. Neurosci.* **26,** 565–597 (2003).
6. Fukamauchi, F. *et al.* TAG1-deficient mice have marked elevation of adenosine A1 receptors in the hippocampus. *Biochem. Biophys. Res. Commun.* **281,** 220–226 (2001).
7. Cao, X. & Sudhof, T. C. A transcriptively active complex of APP with Fe65 and histone acetyltransferase Tip60. *Science* **293,** 115–120 (2001).
8. King, G. D. & Turner, R. S. Adaptor protein interactions: modulators of amyloid precursor protein metabolism and Alzheimer's disease risk? *Exp. Neurol.* **185,** 208–219 (2004).
9. Chang, Y. *et al.* Generation of the β-amyloid peptide and the amyloid precursor protein C-terminal fragment gamma are potentiated by FE65L1. *J. Biol. Chem.* **278,** 51100–51107 (2003).
10. Tanahashi, H. & Tabira, T. Characterization of an amyloid precursor protein-binding protein Fe65L2 and its novel isoforms lacking phosphotyrosine-interaction domains. *Biochem. J.* **367,** 687–695 (2002).
11. Rodier, P. M. Correlations between prenatally-induced alterations in CNS cell populations and postnatal function. *Teratology* **16,** 235–246 (1977).
12. Cao, X. & Sudhof, T. C. Dissection of amyloid-β precursor protein-dependent transcriptional transactivation. *J. Biol. Chem.* **279,** 24601–24611 (2004).
13. Traka, M. *et al.* Association of TAG1 with Caspr2 is essential for the molecular organization of juxtaparanodal regions of myelinated fibers. *J. Cell Biol.* **162,** 1161–1172 (2003).
14. Chen, S., Mantei, N., Dong, L. & Schachner, M. Prevention of neuronal cell death by neural adhesion molecules L1 and CHL1. *J. Neurobiol.* **38,** 428–439 (1999).
15. Hemann, C., Gartner, E., Weidle, U. H. & Grummt, F. High-copy expression vector based on amplification-promoting sequences. *DNA Cell Biol.* **13,** 437–445 (1994).
16. Zheng, H. *et al.* β-Amyloid precursor protein-deficient mice show reactive gliosis and decreased locomotor activity. *Cell* **81,** 525–531 (1995).
17. Wang, B. *et al.* Isoform-specific knockout of FE65 leads to impaired learning and memory. *J. Neurosci. Res.* **75,** 12–24 (2004).
18. Ando, K., Iijima, K. I., Elliott, J. I., Kirino, Y. & Suzuki, T. Phosphorylation-dependent regulation of the interaction of amyloid precursor protein with Fe65 affects the production of beta-amyloid. *J. Biol. Chem.* **276,** 40353–40361 (2001).
19. Hebert, S. S. *et al.* Regulated intramembrane proteolysis of amyloid precursor protein and regulation of expression of putative target genes. *EMBO Rep.* **7,** 739–745 (2006).
20. Vingtdeux, V. *et al.* Alkalizing drugs induce accumulation of amyloid precursor protein by-products in luminal vesicles of multivesicular bodies. *J. Biol. Chem.* **282,** 18197–18205 (2007).

© 2008 Nature Publishing Group

nature cell biology

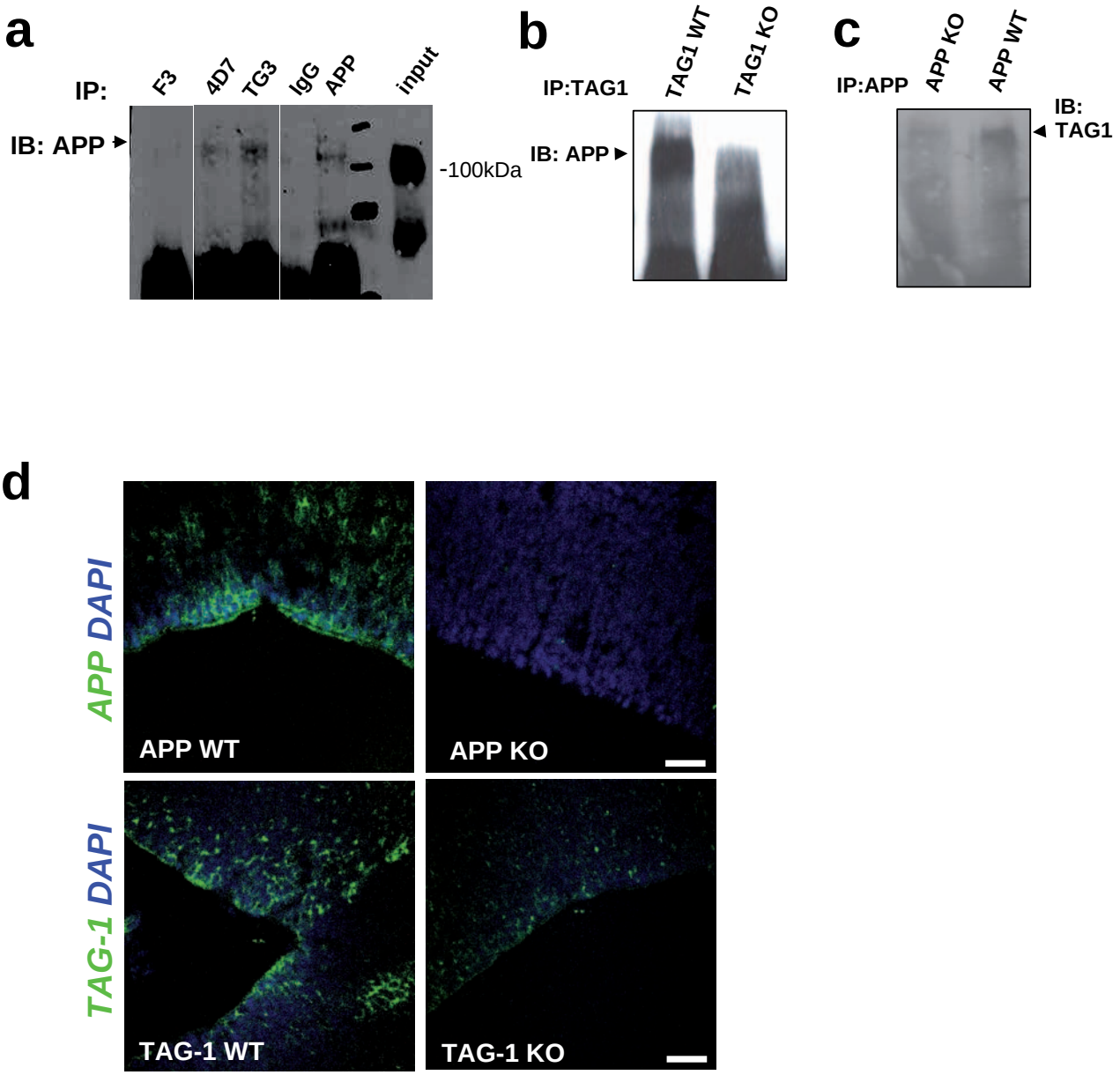

Figure S1 Interaction between APP and TAG1. Co-immunoprecipitation of APP with TAG1 (**a**, **b**, and **c**). Brain lysates of wild-type mice were immunoprecipitated using antibodies against TAG1 (4D7 and TG3), F3, and APP as well as non-immune IgG and probed with anti-APP antibody (22c11; **a**). Brain lysates of *TAG1*$^{+/+}$ (TAG1 WT) and *TAG1*$^{-/-}$ (TAG1 KO) mice were immunoprecipitated using antibody against TAG1 (TG1) and probed with anti-APP antibody (22C11; **b**). Brain lysates of APP$^{+/+}$ (APP WT) and APP$^{-/-}$ (APP KO) mice were immunoprecipitated using antibody against APP (171610) and probed with anti-TAG1 antibody (TG1; **c**). Double immunostaining for APP (green; C7 APP antibody) or TAG1 (green; TG1 antibody) with DAPI (blue) in the walls of the lateral ventricles in E14 *TAG1*$^{-/-}$ and *APP*$^{-/-}$ mouse brain (**d**). Scale bars represent 20 μm.

© 2008 Nature Publishing Group

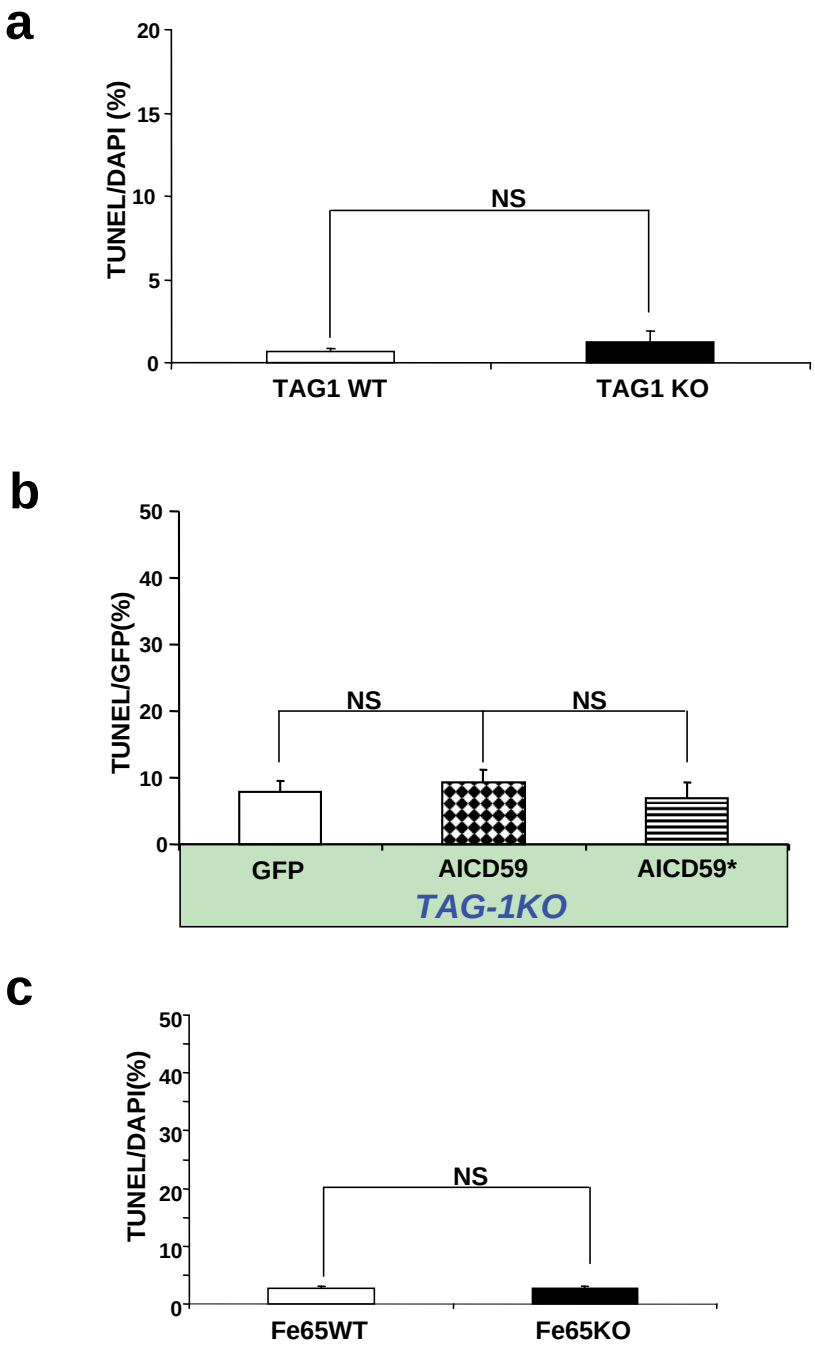

Figure S2 TAG1-APP signaling pathway via Fe65 does not induce apoptosis during neurogenesis. **a**. NPCs were isolated from *TAG1*$^{-/-}$ (TAG1KO) and *TAG1*$^{+/+}$ (TAG1WT). After 7-8 days in vitro culture differentiation, the cells were double-stained for TUNEL and GFP. The number of TUNEL positive cells were counted and expressed as a percentage of the total number of DAPI positive cells. Compared to the control vector group, there were no detectable differences. The numbers of apoptotic cells are very low in the NPCs isolated from *TAG1*$^{-/-}$ and *TAG1*$^{+/+}$ mice (1.20+0.74%and 0.65+0.23%, respectively; mean ± sem). **b.** Expression of Fe65 can lead to the stabilization and nuclear translocation of AICD, where it may induce apoptosis[2,3,4]. To investigate whether overexpression of AICD induces apoptosis in *TAG1*$^{-/-}$ NPCs, NPCs were isolated from *TAG1*$^{-/-}$ (TAG1KO) and transfected with AICD59, AICD mutant (with the NPTY to NATA mutation; AICD59*) and GFP (AICD59) and or empty vector containing only GFP (GFP) as a control. After 7-8 days in vitro culture differentiation, the cells were double-stained for TUNEL and GFP. The number of TUNEL positive cells were counted and expressed as a percentage of the total number of GFP positive cells. Compared to the control vector group, there were no detectable differences. **c**. Furthermore, NPCs were isolated from *Fe65*$^{+/+}$ (Fe65WT) and *Fe65*$^{-/-}$ (Fe65KO) mice. After 7-8 days in vitro culture differentiation, the cells were double-stained for TUNEL and DAPI. The number of TUNEL positive cells were counted and expressed as a percentage of the total number of DAPI positive cells. The numbers of apoptotic cells are very low in the NPCs isolated from *Fe65*$^{-/-}$ and *Fe65*$^{+/+}$ mice (2.77 ± 0.26% and 2.66 ± 0.36%, respectively; mean ± sem). These observations demonstrate that apoptosis may not be involved in the neurogenesis mediated by the TAG1-APP signaling pathway via Fe65.

© 2008 Nature Publishing Group

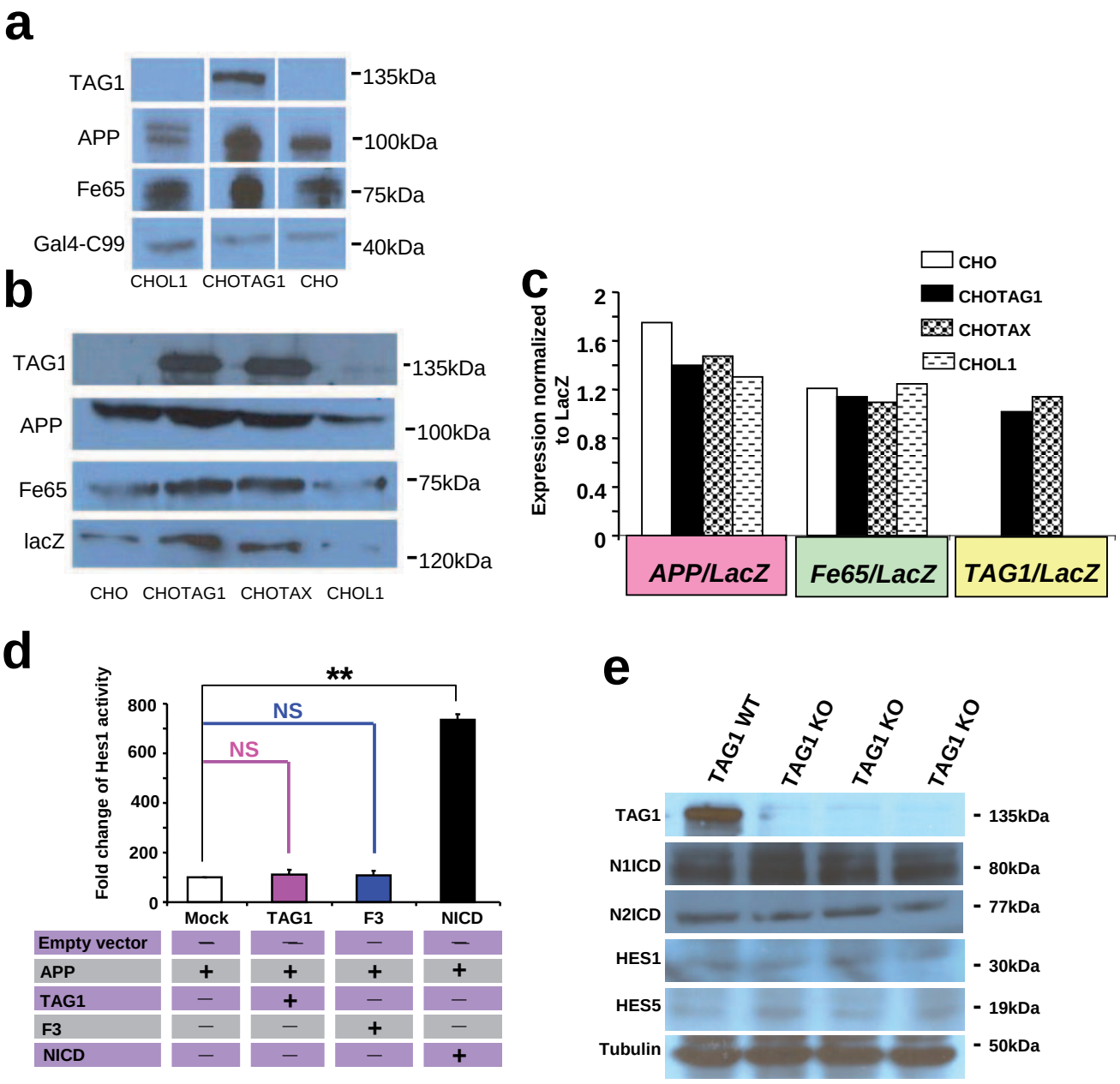

Figure S3 TAG1 and the APP and Notch signaling pathways. **a**, **b**, and **c**. CHO cells and L1 (CHOL1), TAX (CHOTAX) and TAG1 (CHOTAG1) transfected CHO cells were transiently co-transfected in 24-well culture dishes with pG5E1B plasmid, APP-Gal4-responsive luciferase reporter gene, Fe65 plasmid, and luciferase internal control plasmid or pcDNA3.1-lacZ-myc. After normalization to internal control (**a**), whole-cell lysates were subjected to SDS PAGEs and Western blots using antibodies against TAG1 (TG1), APP (22C11), Fe65 (3H6), and Gal4 (630403). Normalization to LacZ-myc, another loading control that was detected by antibodies against myc, is presented in **c**. **a** and **b** present two individual experiments. **d**. Hes1 luciferase reporter activity was affected by neither TAG1 nor F3. NICD transcriptional activity is not triggered by TAG1. CHO cells were transiently co-transfected in 24-well culture dishes with pGVB-Hes1 luciferase reporter plasmid, luciferase internal control plasmid and TAG1 cDNA, F3 cDNA or NICD cDNA as well as empty vector as a control (Mock). Normalized luciferase activities in whole-cell lysates were determined in triplicate and expressed relative to activity in lysates prepared from mock-transfected CHO cells. **e**. There were also no detectable differences between the brains of *TAG1*$^{+/+}$ and *TAG1*$^{-/-}$ mice in Western blot analysis of the expression levels of NICD of Notch1 and Notch2, Hes1 and Hes5. Brain lysates of *TAG1*$^{+/+}$ (WT) and *TAG1*$^{-/-}$ (KO) mice were Western blotted using antibodies against TAG1 (TG1), Notch1 NICD (N1ICD, ab8925), Notch2 NICD (N2ICD, ab8926), Hes1 (AB5702), Hes5 (ab25374) and γ-Tubulin.

© 2008 Nature Publishing Group

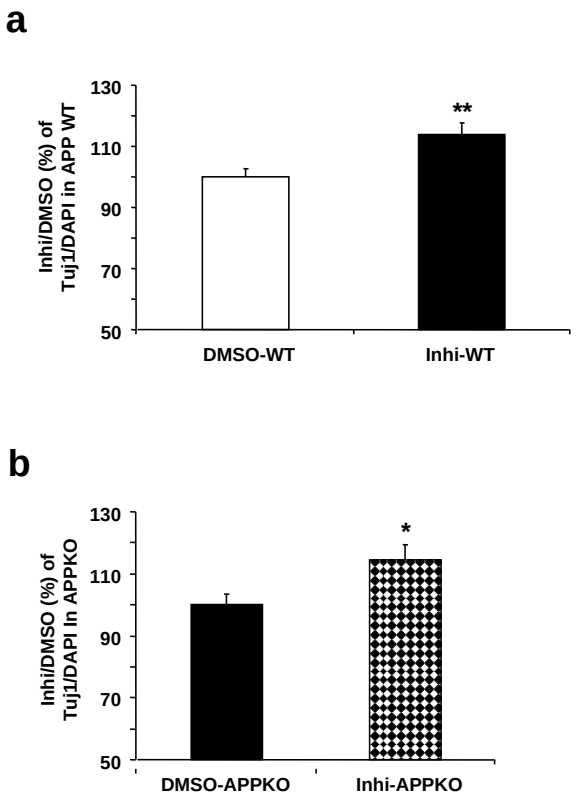

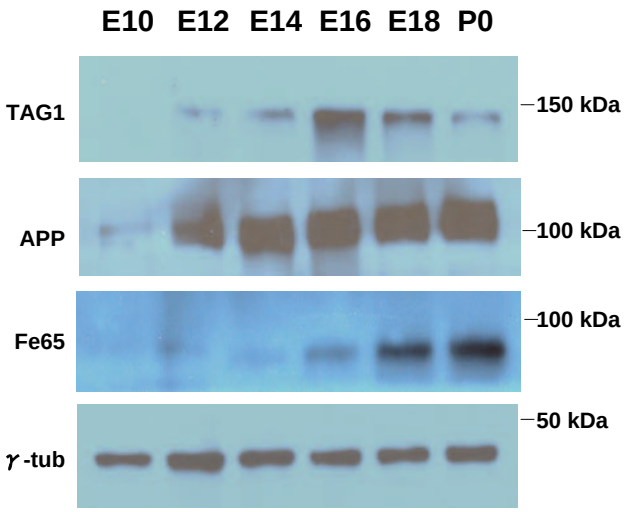

Figure S4 Effects of γ-secretase inhibitor (L-685,458) on neurogenesis. To investigate the effect of a γ-secretase inhibitor on neurogenesis, we treated (**a**) *APP*$^{+/+}$ and (**b**) *APP*$^{-/-}$ NPCs with L-685,458 (20μM) and DMSO as a control. After 7-8 days in vitro culture differentiation, the cells were double-stained for TUJ1 and DAPI. The number of TUJ1 positive neurons were counted and expressed as a percentage of the total number of DAPI positive neurons normalized to the DMSO control condition (* $p<0.05$; ** $p<0.001$. Error bars represent SEM). Notably, the neurogenesis in both *APP*$^{-/-}$ and *APP*$^{+/+}$ NPCs was significantly increased. These observations demonstrate that γ-secretase plays a role in neurogenesis. Given that presenilins mediate the regulated intramembrane proteolysis of a number of transmembrane proteins, such as Notch, APP, and ErbB-4, which release soluble intracellular domains that carry out different signaling functions[5,6], these results do not demonstrate that APP is essential as they do not indicated through which signaling pathway this effect is mediated in the presence of APP. However, we have confirmed that two γ-secretase inhibitors, L-685,458 and DAPT, have similar effects on downregulation of the luciferase activity induced by the TAG1-APP interaction (**Fig. 4b, c,** and f; **Fig. 7a**). This demonstrates that the TAG1-APP signaling pathway is dependent on γ-secretase.

Figure S5 Developmental expression of TAG1, APP and Fe65. Moreover, we investigated developmental expression of APP, TAG1 and Fe65. Whole brain protein lysates from E10, E12, E14, E16, E18 and P0 mouse brain were Western blotted with antibodies against TAG1 (TG1), APP (A8717) and Fe65 (3H6).

© 2008 Nature Publishing Group

Fig. 1c

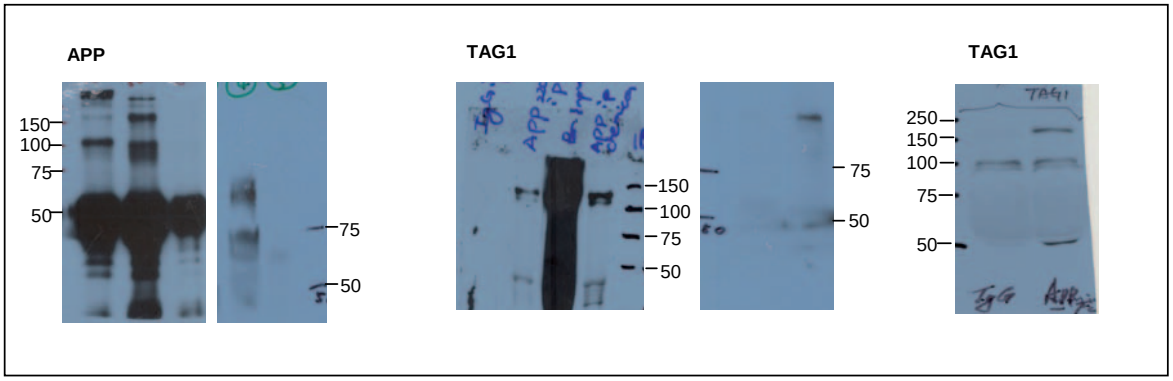

Fig. 1d

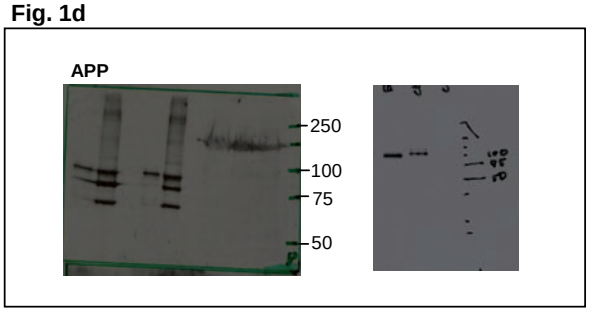

Fig. 1e

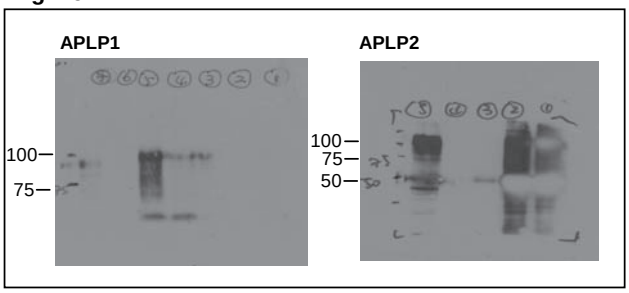

Fig. 2g

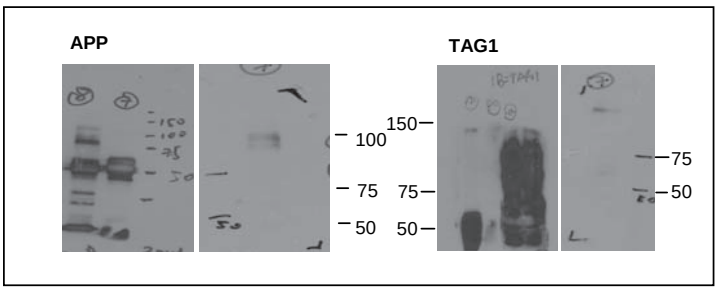

Fig. S1a

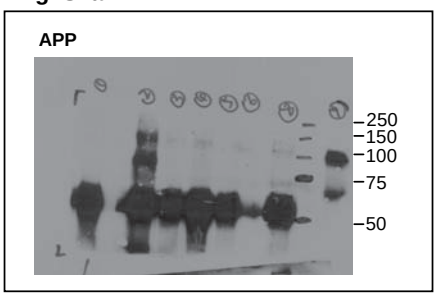

Fig. 5d

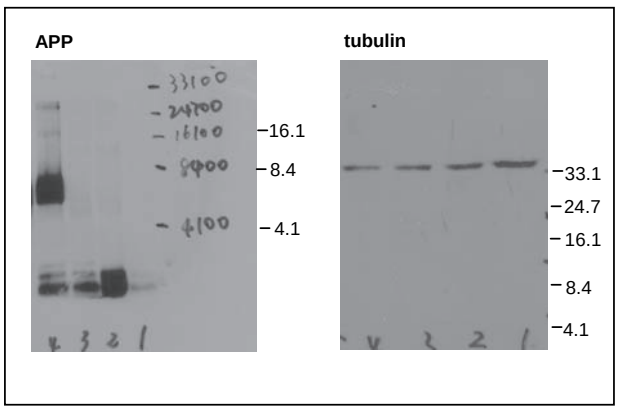

Fig. S1b

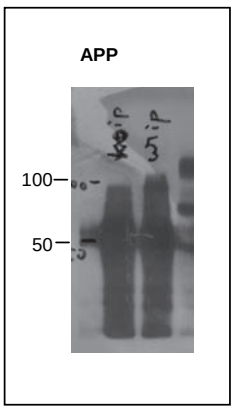

Fig. S1c

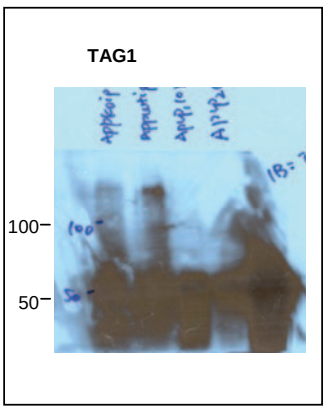

Figure S6 Full scans of Western blots presented in Figures: 1c, d, and e, 2g, 4, 5d, S1a, b and c.

© 2008 Nature Publishing Group

SUPPLEMENTARY EXPERIMENTAL PROCEDURES

Production of the APP-Fc fusion protein

Mouse APP 695 cDNA encoding for the neuronal isoform of APP (from Dr S. Sisodia) was subcloned into the pblue Bac vector using the BamHI and SacI restriction sites. To generate the fusion protein containing the extracellular domain of APP with the Fc part of human immunoglobulin G at its COOH-terminal end (APP-Fc), primers for the SacI restriction site at the 5´end (CTGACGGAACCAAGACCACCG) and for the COOH terminal end of the APP extracellular domain (terminating at amino acid position 624; SWISS-Prot accession number P12023) at the 3´ end (GCTGAAGATGTGGGTTCGAACAAA) were used, introducing a new BclI restriction site at the 3´end.

Cell adhesion assay

CHO cells were stably transfected with pcDNA 3.1(-) containing the mouse cDNA sequence of APP 695. APP-, F3-, TAX-, TAG1- and mock-transfected CHO cells were cultured in DMEM containing 10% fetal calf serum. Thirty-five mm tissue culture petri dishes (Becton Dickinson, Franklin Lakes, NJ USA) were coated with methanol-solubilized nitrocellulose and then with proteins (12 μM) for 2 hrs at 37^{o}C in a humidified atmosphere. Subsequently, the dishes were washed and blocked overnight with 2% heat-inactivated fatty acid-free BSA (Sigma-Aldrich). After rinsing the dishes, cells (TAG1-transfected CHO or APP-transfected CHO) were plated in 2 ml of DMEM (Gibco, Invitrogen, Carlsbad, CA, USA) containing 10% fetal calf serum at a density of 1.5 x 10^{6}cells/ml. At 0.5 hr (in the adhesion test), the cells were gently washed and fixed with 2.5% glutaraldehyde and stained with 0.5% toluidine blue (Sigma-Aldrich) in 2.5% sodium carbonate. Blockage of adhesion was carried out using polyclonal anti-TAG1 (1:100) or anti-APP (1:100) antibodies for 0.5 h pre-incubation. Cells adhering to the various spots were photographed and counted. The results were analyzed by Newman-Keuls test with $p<0.05$ being considered significant.

Immunocytochemistry and quantification

© 2008 Nature Publishing Group

Immunocytochemistry on cultured cells and immunostaining of tissue sections were performed as previously described[15 (in text)]. For quantification of immunofluorescence, images of fields of cultured cells were captured by digital photomicrograph under a 10X objective systematically from top-to-bottom and left-to-right across the entirety of each coverslip. All labeled cells were then counted in each photomicrograph. The proportion of neurons was quantified as the numbers of Tuj1+ or MAP2+ cells divided by the total number of DAPI+ cells in the same fields. Each experiment was repeated on 3 to 7 mice. The statistics were performed using one-way-ANOVA or Student's t test, as appropriate. In all the graphs, the error bars indicate standard error of the mean (SEM). *: $P<0.05$; **: $P<0.001$.

Luciferase assay

The APP-Gal4 assay system has been previously described[7 (in text)]. L1-, TAG1- and TAX-transfected CHO cells as well as CHO cells were co-transfected with the following plasmids (i) pG5E1B-luc (Gal4 reporter plasmid, 0.1 μg DNA); (ii) pCMV-LacZ (β-galactosidase control plasmid, 0.05 μg DNA); (iii) pMstAPP (Gal4) or pMstC99 (Gal4) (0.1 μg DNA); (iv) pCMV5-Fe65 (Fe65) (0.1 μg DNA), in 24-well dishes using an Effectene Transfection kit (Qiagen, Valencia, CA, USA). Additionally, cells cultured in 24-well dishes were used for AICD-Gal4, C99-Gal4, APP*-Gal4 (with NPTY to NATA mutation), AICD59*-Gal4 (with NPTY to NATA mutation), and Fe65-Gal4 luciferase reporter assays. For the transactivation assay in NPCs, wells were coated with L1-Fc, TAG1-Fc, F3-Fc or laminin protein (8 nM). Each well received 10 times the amount of DNA as used for the CHO cells and the transfection was performed using a Nucleofector System (amaxa Biosystems, Gaithersburg, MD, USA). To examine the role of γ–secretase in this tansactivation, different concentrations of γ–secretase inhibitors (L-685, 458: 2 or 4μM; DAPT: 10, 20, 30, or 40μM; Calbiochem) were applied to tansfected cells, while DMSO was used as a control. The β-galactosidase expression plasmid pCMV-β-Gal was included to monitor the transfection efficiency. Cells were lysed at 24 hrs after transfection and assayed using the Steady-Glo Luciferase Assay Kit (Promega, Madison, WI, USA). The Hes1 luciferase reporter assay has been previously described[4 (in text)].

© 2008 **Nature Publishing Group**

Western blotting for AICD detection in CHO and MEF cells and E15 mouse brain

Protein extraction for detection of AICD in cell lines was as previously described[18, 19 (in text)]. APP-transfected CHO cells were co-transfected with cDNAs of Fe65, PS1 and TAG1 or pRC vector as control or CHO cells were co-transfected with cDNAs of APP-V5, Fe65, BACE1 and TAG1 or pRC vector as control. After transfection, cells were cultured in DMEM (Gibco) for 24 h and 20mM NH_4Cl was added[1] into the medium for culture for another 24h. MEF cells were transfected with 1 μg, 2.5 μg or 5 μg of pRC-TAG1 vector or 2.5 μg empty pRC vector as control and collected 48 h after transfection or MEF cells were treated for 3 hr at 37 ^{o}C with recombinant human TAG1 (R&D systems, USA) or recombinant human F3-Fc (R&D systems). Total proteins were prepared by direct extraction in Tricine sample buffer (Bio-Rad Laboratories) containing a protease inhibitor cocktail (Roche), sonication and boiling for 5 min. The proteins were loaded onto 16% SDS-Tricine polyacrylamide gel and transferred onto PVDF membranes.

Protein extraction to detect AICD in mouse brain was as previously described[20 (in text)]. Briefly, E15 mice brains were homogenized and sonicated in buffer (20mM HEPES-NaOH (pH 7.4), 150 mM NaCl, 10% glycerol, 5 mM EDTA, 20 mM NH4Cl) containing 0.5% TritonX-100, 5mg/ml chymostatin, and 5mg/ml leupeptin, and incubated on ice for 15 min, centrifuged at 16000 X g for 15 min and boiled for 5 min. Protein levels were quantified (Bio-Rad Laboratories). The protein was applied to 12% SDS-Tricine polyacrylamide gels and transferred onto PVDF membranes.

The PVDF membranes were warmed by intermittent microwave irradiation (5 x 10 s irradiation at 5 min intervals). The PVDF membranes were blocked with 5% dry fat milk in TBST plus 0.05% Tween 20 and incubated with primary antibodies against the C-terminal of APP (A8717, Sigma-Aldrich), TAG1 (TG1 from Dr Watanabe) and γ-tubulin (Sigma-Aldrich) in TBST containing 5% dry fat milk overnight at 4 ^{o}C and for 1h at room temperature. The membranes were washed with TBST and incubated with horseradish peroxidase-conjugated sheep anti-mouse IgG or donkey anti-rabbit IgG

© 2008 Nature Publishing Group

(Amersham Biosciences) for 2h at room temperature. ECL Plus or ECL Advance Western Blotting Detection Reagents (Amersham Biosciences) were used to visualize the immunoreactive proteins. Loading controls between Western blot lanes were normalized according to the γ-tubulin signal.

SUPPLEMENTARY DISCUSSION

We first showed that TAG1 and APP bind to each other in cell adhesion assays using a system in which the proteins were overexpressed in CHO cells. We also investigated TAG1 and APP binding by co-immunoprecipitation and pull-down assays. In extracts from wild-type brain, antibodies to TAG1 could precipitate APP, and vice versa. There was no co-immunoprecipitation in samples from *APP*$^{-/-}$ and *TAG1*$^{-/-}$ mice suggesting that the interaction was specific. We next showed that TAG1 and APP co-localize in the neurogenic niche of the ventricular zone in the developing mouse brain and within NPCs isolated from this region. NPCs isolated from *TAG1* null and *APP* null mice showed abnormally enhanced neurogenesis, suggesting that TAG1 and APP are involved in negative regulation of neurogenesis. This is consistent with increasing evidence that has suggested potential roles for both APP and TAG1 in the development of neural stem cells. APP mRNA transcripts can be detected in mouse oocytes and early in mouse embryogenesis[7], such as in the mouse neural tube on E9.5, a stage when the neural stem cells and RC2-positive radial glia are actively dividing[8]. APP is expressed by neuroepithelial cells of the cortical ventricular zone, particularly in the apical portion where mitosis takes place at E14 to E16[9]. Moreover, secreted N-terminal nonamyloidogenic APP acts as an EGF cofactor to stimulate proliferation of the cells from embryonic neurospheres *in vitro* and its major binding sites locate on the surface of type-A and -C cells in the SVZ[10]. Similarly, the expression of TAG1 appears early in development, for example on the cell bodies of motor neurons in spinal cord at E10.5 and during their lateral migration from the ventricular zone at E13[2 (in text)]. Thus, our data link the existing evidence for roles for TAG1 and APP in neural development, showing that TAG1 and APP are involved in negative modulation of neurogenesis. Notably, if TAG1 and APP suppressed neurogenesis by independent mechanisms, it might be expected that the effects of knocking out TAG1 and APP would be additive. However, NPCs from

© 2008 **Nature Publishing Group**

TAG1&APP double null mice showed a similar enhancement in neurogenesis to NPCs from single *TAG1* and *APP* null mice, suggesting that the mechanisms by which TAG1 and APP reduce neurogenesis are convergent.

What are the mechanisms underlying the role of TAG1-APP signaling in modulation of neurogenesis? The interaction between TAG1 and APP is reminiscent of the RIP of Notch signaling cascade after F3 stimulation[4] [(in text)]. The observation that TAG1 stimulated AICD-dependent luciferase reporter activity showed that TAG1-triggers AICD release. That there is AICD-dependent luciferase reporter activity in this system is consistent with the concept that the intracellular fragments of type-1 transmembrane proteins, such as Notch, are released by RIP[1] [(in text)]. We further showed that TAG1 can trigger AICD release in a γ-secretase-dependent manner. Using APP-transfected CHO cells transfected with cDNAs of Fe65, PS1 and TAG1 and CHO cells co-transfected with cDNAs of APP-V5, Fe65, BACE1 and TAG1, we have shown that TAG1 significantly increases AICD release, which could be blocked by a γ-secretase inhibitor. Moreover, we also showed that endogenous AICD production in MEF cells is dose-dependently increased by transfection with TAG1 or treatment with TAG1 but not by treatment with F3-Fc. Consistently, endogenous AICD production was reduced in embryonic *TAG1* null mouse brains compared to wild-type mice. In addition to the γ-secretase-dependent AICD production, both CTF-α and CTF-β increased dose-dependently in response to TAG1 *in vitro*, suggesting that both α- and β-secretase cleavage can be stimulated by TAG1. The presence of both extracellular and intramembrane cleavages triggered by the interaction between TAG1 and APP is consistent with the characteristic features of RIP.

However, the transcriptional activity of the AICD product cleaved from APP has been controversial. It was reported that binding to Fe65 stabilizes AICD and that both Fe65 and AICD translocate to the nucleus[11]. AICD appeared to have transcriptional activity in complex with Fe65 and histone acetyltransferase Tip60[7] [(in text)]. However, this transcriptional activity was in the same artificial reporter gene assay that we used in the present study. This artificial reporter assay system can detect release of AICD tagged

© 2008 **Nature Publishing Group**

with Gal4 but, as the response element is Gal4, activity in this system does not reflect endogenous transcriptional activity of AICD. Whether AICD is involved in endogenous transcriptional activation remains to be further investigated. Moreover, the role of AICD in the mechanisms of the transcriptional activation has also been controversial. Early evidence suggested that Fe65 bound to APP and that when AICD was cleaved the two proteins translocated to the nucleus together[7 (in text), 11] complexing with Tip60[7 (in text)]. Later evidence indicated that membrane-tethered AICD recruits and activates Fe65 allowing its translocation to the nucleus but that it is not essential for Fe65-dependent transcriptional transactivation[12 (in text)]. Moreover, a subsequent study confirmed that Fe65 alone was sufficient for transcriptional transactivation and that APP and Tip60 play positive and negative modulatory roles, respectively[12]. Investigation of the phosphorylation of APP at Thr688 (residue numbering for the APP695 form), which reduces or prevents Fe65 binding to APP[13] and disrupts the stabilization of AICD by Fe65 binding[14], suggested that activation of Fe65 may involve liberation from membrane bound APP on phosphorylation and that unphosphorylated, but not phosphorylated, AICD translocates to the nucleus independently of Fe65[15]. Yet, despite the growing evidence that AICD is necessary for neither the transcriptional activity of Fe65 nor its translocation to the nucleus, several recent studies have suggested that AICD can regulate transcription of endogenous genes, including *KAI1*, *GSK-3β*, *APP*, *BACE*, *neprilysin*, *α2-actin*, *transgelin*, and *EGFR*[1,16-20], although the transcriptional control of *KAI1*, *GSK-3β*, *APP* and *neprilysin* have been controversial[21-23]. In the case of the epidermal growth factor receptor (EGFR), direct binding of endogenous AICD to the *EGFR* promoter is reported[20]. It has also been suggested that AICD can enhance the transcriptional activation of another transcription factor, p53[24]. Thus, despite the controversy over whether AICD is itself a transcription factor in the AICD-Fe65-Tip60 system, there is growing evidence that AICD can influence gene transcription. It is therefore of interest to understand the regulation of AICD cleavage. Our finding that TAG1 can stimulate AICD-dependent activity in a γ-secretase dependent manner in the artificial luciferase reporter system is evidence that TAG1 can act as a functional ligand for APP.

© 2008 **Nature Publishing Group**

Importantly, we went on to show that both AICD and Fe65 are necessary for the TAG1-APP-dependent negative modulation of neurogenesis. Application of soluble TAG1 or transfection with AICD59, but not mutant AICD59*, reversed the abnormal neurogenesis in NPCs from *TAG1* null mice, but TAG1 could not reverse the abnormal neurogenesis in NPCs from *TAG1&APP* double null mice. Moreover, soluble TAG1 decreased neurogenesis in NPCs from wild-type mice but could not reverse the increased neurogenesis seen in *Fe65* null mice. Consistently, a γ-secretase inhibitor increased neurogenesis in NPCs from wild-type mice. However a similar effect was also seen in NPCs from *APP* null mice indicating that other γ-secretase-dependent pathways are also involved in regulation of neurogenesis in NPCs. Although there is continuing controversy over whether AICD is itself a modulator of transcription, our data indicate that TAG1 acts as an APP ligand to negatively modulate neurogenesis via a pathway that depends upon AICD and Fe65. In Alzheimer's disease (AD), proteolytic processing of APP by β- and γ-secretases leads to the accumulation of insoluble Aβ fragments[25]. Although Aβ and AICD production do not appear to be tightly linked[26], altered APP processing may influence AICD production or lead to formation of alterative C-terminal products[27], which could have implications for physiological signaling via the AICD-dependent TAG1-APP signaling pathway. TAG1 did appear to increase both production of both CTF-α and CTF-β. It would however be overly speculative at this stage to draw parallels between our finding that TAG1-APP signaling negatively modulates neurogenesis in NPCs isolated from the fetal mouse cortex and the reported increase in neurogenesis in an AD mouse model[28] and the adult human hippocampus in AD[29]. Not only do the mechanisms regulating neurogenesis differ between fetal and adult brain and between hippocampus and cortex, but also the changes in neurogenesis in AD and their implications are controversial[30].

In summary, we have shown that TAG1, a member of the F3 family, is a functional ligand of APP. Similar to F3 triggered NICD activity[4 (in text)], this ligand binding promotes AICD release in a γ-secretase-dependent manner. Moreover, we have demonstrated that the TAG1-APP signaling pathway through Fe65 negatively modulates neurogenesis. Importantly, the increase in neurogenesis observed in neural stem cells

© 2008 **Nature Publishing Group**

isolated from *TAG1* null mice was reversed by expression of AICD, confirming that negative modulation of neurogenesis is a physiological role of cleaved AICD. These findings are important in the context of Alzheimer's disease because abnormal processing of APP could also lead to aberrant AICD generation, which may be linked to abnormal intracellular signaling. Further research is required to understand the details of the mechanisms by which the TAG1-APP signaling pathway as well as its downstream elements modulate neural stem cells. Knowledge of these mechanisms will provide insights into the cellular processes of neurodegenerative disease and may also offer unique opportunities for pharmacological intervention.

SUPPLEMNTARY REFERENCES

1. Muller,T. *et al.* Modulation of gene expression and cytoskeletal dynamics by the amyloid precursor protein intracellular domain (AICD). *Mol. Biol. Cell* **18**, 201-210 (2007).

2. Kimberly, W. T., Zheng, J. B., Guenette, S. Y., and Selkoe, D. J. (2001). The intracellular domain of the beta-amyloid precursor protein is stabilized by Fe65 and translocates to the nucleus in a Notch-like manner. J. Biol. Chem. 276, 40288–40292.

3. Kinoshita A, Whelan CM, Berezovska O, Hyman BT. (2002) The gamma secretase-generated carboxyl-terminal domain of the amyloid precursor protein induces apoptosis via Tip60 in H4 cells. J Biol Chem. 277, 28530-28536.

4. Kinoshita A, Whelan CM, Smith CJ, Berezovska O, Hyman BT. (2002) Direct visualization of the gamma secretase-generated carboxyl-terminal domain of the amyloid precursor protein: association with Fe65 and translocation to the nucleus. J Neurochem. 82, 839-847.

© 2008 **Nature Publishing Group**

5. Ebinu, J. O. and Yankner, B. A. (2002). A RIP tide in neuronal signal transduction. Neuron 34, 499-502.

6. Koo EH, Kopan R. (2004) Potential role of presenilin-regulated signaling pathways in sporadic neurodegeneration. Nat Med. 10 S26-33.

7. Fisher,S., Gearhart,J.D. & Oster-Granite,M.L. Expression of the amyloid precursor protein gene in mouse oocytes and embryos. *Proc. Natl. Acad. Sci. U. S. A* **88**, 1779-1782 (1991).

8. Salbaum,J.M. & Ruddle,F.H. Embryonic expression pattern of amyloid protein precursor suggests a role in differentiation of specific subsets of neurons. *J Exp. Zool.* **269**, 116-127 (1994).

9. Lopez-Sanchez,N., Muller,U. & Frade,J.M. Lengthening of G2/mitosis in cortical precursors from mice lacking beta-amyloid precursor protein. *Neuroscience* **130**, 51-60 (2005).

10. Caille,I. *et al.* Soluble form of amyloid precursor protein regulates proliferation of progenitors in the adult subventricular zone. *Development* **131**, 2173-2181 (2004).

11. Kimberly,W.T., Zheng,J.B., Guenette,S.Y. & Selkoe,D.J. The intracellular domain of the beta-amyloid precursor protein is stabilized by Fe65 and translocates to the nucleus in a notch-like manner. *J Biol. Chem.* **276**, 40288-40292 (2001).

12. Yang,Z., Cool,B.H., Martin,G.M. & Hu,Q. A dominant role for FE65 (APBB1) in nuclear signaling. *J Biol. Chem.* **281**, 4207-4214 (2006).

13. Ando,K., Iijima,K.I., Elliott,J.I., Kirino,Y. & Suzuki,T. Phosphorylation-dependent regulation of the interaction of amyloid precursor protein with Fe65 affects the production of beta-amyloid. *J Biol. Chem.* **276**, 40353-40361 (2001).

© 2008 **Nature Publishing Group**

14. Kimberly,W.T., Zheng,J.B., Town,T., Flavell,R.A. & Selkoe,D.J. Physiological regulation of the beta-amyloid precursor protein signaling domain by c-Jun N-terminal kinase JNK3 during neuronal differentiation. *J Neurosci.* **25**, 5533-5543 (2005).

15. Nakaya,T. & Suzuki,T. Role of APP phosphorylation in FE65-dependent gene transactivation mediated by AICD. *Genes Cells* **11**, 633-645 (2006).

16. Baek,S.H. *et al.* Exchange of N-CoR corepressor and Tip60 coactivator complexes links gene expression by NF-kappaB and beta-amyloid precursor protein. *Cell* **110**, 55-67 (2002).

17. Kim,H.S. *et al.* C-terminal fragments of amyloid precursor protein exert neurotoxicity by inducing glycogen synthase kinase-3beta expression. *FASEB J* **17**, 1951-1953 (2003).

18. Pardossi-Piquard,R. *et al.* Presenilin-dependent transcriptional control of the Abeta-degrading enzyme neprilysin by intracellular domains of betaAPP and APLP. *Neuron* **46**, 541-554 (2005).

19. von Rotz,R.C. *et al.* The APP intracellular domain forms nuclear multiprotein complexes and regulates the transcription of its own precursor. *J Cell Sci.* **117**, 4435-4448 (2004).

20. Zhang,Y.W. *et al.* Presenilin/gamma-secretase-dependent processing of beta-amyloid precursor protein regulates EGF receptor expression. *Proc. Natl. Acad. Sci. U. S. A* **104**, 10613-10618 (2007).

21. Chen,A.C. & Selkoe,D.J. Response to: Pardossi-Piquard et al., "Presenilin-Dependent Transcriptional Control of the Abeta-Degrading Enzyme Neprilysin by Intracellular Domains of betaAPP and APLP." *Neuron* **53**, 479-483 (2007).

22. Hebert,S.S. *et al.* Regulated intramembrane proteolysis of amyloid precursor protein and regulation of expression of putative target genes. *EMBO Rep.* **7**, 739-745 (2006).

© 2008 **Nature Publishing Group**

23. Pardossi-Piquard,R. *et al.* Response to Correspondence: Pardossi-Piquard et al., "Presenilin-Dependent Transcriptional Control of the Abeta-Degrading Enzyme Neprilysin by Intracellular Domains of betaAPP and APLP." Neuron 46, 541-554. *Neuron* **53**, 483-486 (2007).

24. Ozaki,T. *et al.* The intracellular domain of the amyloid precursor protein (AICD) enhances the p53-mediated apoptosis. *Biochem. Biophys. Res. Commun.* **351**, 57-63 (2006).

25. Selkoe,D.J. Alzheimer's disease: genes, proteins, and therapy. *Physiol Rev.* **81**, 741-766 (2001).

26. Hecimovic,S. *et al.* Mutations in APP have independent effects on Abeta and CTFgamma generation. *Neurobiol. Dis.* **17**, 205-218 (2004).

27. Evin,G., Zhu,A., Holsinger,R.M., Masters,C.L. & Li,Q.X. Proteolytic processing of the Alzheimer's disease amyloid precursor protein in brain and platelets. *J Neurosci. Res.* **74**, 386-392 (2003).

28. Jin,K. *et al.* Enhanced neurogenesis in Alzheimer's disease transgenic (PDGF-APPSw,Ind) mice. *Proc. Natl. Acad. Sci. U. S. A* **101**, 13363-13367 (2004).

29. Jin,K. *et al.* Increased hippocampal neurogenesis in Alzheimer's disease. *Proc. Natl. Acad. Sci. U. S. A* **101**, 343-347 (2004).

30. Kuhn,H.G., Cooper-Kuhn,M., Boekhoorn,K. & Lucassen,P.J. Changes in neurogenesis in dementia and Alzheimer mouse models: are they functionally relevant? *Eur. Arch. Psychiatry Clin. Neurosci.* (2007).

© 2008 **Nature Publishing Group**